

Geomorphological consequences of weak lower continental crust, and its significance for studies of uplift, landscape evolution, and the interpretation of river terrace sequences

R. Westaway

16 Neville Square, Durham DH1 3PY, England

Received: January 2001; accepted: February 2002



Abstract

Effects of flow in the lower continental crust have often been ignored in the geomorphological literature on the growth of topography during the Quaternary. However, the ability of the lower crust to flow in response to horizontal pressure gradients, caused by lateral variations in the depth of the base of the brittle upper crust, results in two mechanisms for the growth of topography, which can occur either separately or in combination. First, an increase in the rate of erosion in a region will result in a progressive reduction in the depth of the base of the brittle layer, which will drive inflow of lower crust to beneath the region, which will increase the crustal thickness and thus the altitude of the Earth's surface. It is important to note that this mechanism can increase the mean altitude of the Earth's surface, not just the altitude of summits formed of erosion-resistant rock or other features that are not eroding, which will rise faster than the surrounding eroding landscape. Second, repeated cyclic surface loading by ice sheets or fluctuations in global sea-level will cause net flow from areas of relatively cool lower crust to beneath areas of warmer crust. This process will thus usually result in net flow of lower crust from beneath offshore areas to beneath land areas, thinning the crust and increasing the bathymetry offshore but adding to the crustal thickness and so uplifting the land surface onshore. Although these two processes have different mechanisms, the time scale over which both operate is governed by the time required for heat diffusion, resulting from lower-crustal flow (which is concentrated near the Moho), to affect the position of the base of the brittle layer. As a result, the uplift responses for both processes can be very similar. This means that to resolve the physical cause of uplift at any locality requires knowledge of the regional conditions before uplift began, not just evidence (such as river terrace sequences) from during the course of uplift. This study illustrates the complexities and practical difficulties that can result from these issues, using case studies of localities that have been modelled in detail. It also points out that, although the ability to carry out quantitative calculations involving lower-crustal flow is new, the idea that such flow provides a general mechanism for the growth of topography was first suggested in the early 19th century, but was later abandoned – apparently mistakenly. An early Middle Pleistocene increase in uplift rates is widely-recognised from river terrace records, and typically marks a transition from broad valleys in areas of low relief to narrower, more deeply incised gorges. It is suggested that the isostatic response to cyclic surface loading, caused by the growth and decay of continental ice sheets and the associated sea-level fluctuations, is the main cause of this change, following the increase in scale of ice sheet development from oxygen isotope stage 22 (~0.9 Ma) onwards. The less well resolved earlier increase in uplift rates, evident in some river terrace records at ~3 Ma, is more likely to result from the isostatic response to increased rates of erosion linked to the contemporaneous deterioration in climate.

Key words: Quaternary, river terraces, geomorphology, uplift, erosion

Introduction

The aim of this study is to summarise recent work (from a series of papers including Westaway, 1994a,

1994b, 1995, 1996, 1998, 1999, 2001, 2002a, 2002b, 2002c; Mitchell & Westaway, 1999; Arger et al., 2000; and Westaway et al., 2002) on the role of flow in the lower continental crust in the development of topog-

raphy (Fig. 1), and to highlight its importance in the development and evolution of river valleys during the Quaternary. Others have – of course – also researched this topic since the mid 1980s (e.g., King et al., 1988). However, the resulting literature contains many errors of logic (discussed for instance by Mitchell & Westaway, 1999 and Westaway 2002b; see also below). The present study will therefore be based on the series of references listed above, which are each internally consistent as well as mutually consistent with each other.

The question of whether the altitude of the Earth's surface in onshore areas has systematically increased during the Quaternary has developed major importance. Many studies have claimed, using geomorphological evidence, that this is so (e.g., De Sitter, 1952; King, 1955; Flint, 1957; Geyl, 1960; Holmes, 1965; Damon, 1971; McKee & McKee, 1972; Bond, 1978; Lucchitta, 1979; Partridge & Maud, 1987; Veldkamp, 1996; Eyles, 1996). However, Molnar & England (1990) argued that increasing rates of erosion in the Quaternary, due to the typically harsher climate, can create dissected landscapes in which the local relief is enhanced, causing summit altitudes to increase but with a near-constant mean surface altitude (Fig. 2). This idea has been criticised, for instance by Summerfield & Kirkbride (1992), and it is indeed clear that regions do exist where substantial Quaternary uplift of the land surface has accompanied minimal local erosion. An example is the Rhenish Massif in western Germany (e.g., Westaway, 2001a) where up to ~300 m of Late Pliocene and Quaternary uplift (including, in some localities, ~200 m of uplift since the end of the Early Pleistocene) – estimated from river gorge incision (Fig. 3) – has accompanied negligible spatially-averaged erosion of the local outcrop of

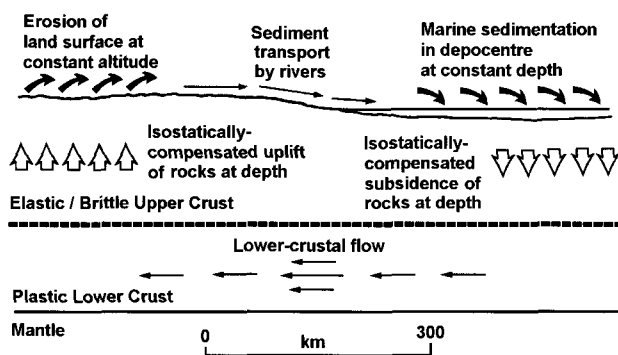


Fig. 1. Cartoon indicating the cyclic transport, under steady-state conditions, of continental crust linking regions of denudation and sedimentation. Horizontal transport of material at the Earth's surface (in this case, by rivers) balances flow in the lower crust in the opposite direction. Redrawn from Westaway (1994b, Fig. 4). The horizontal scale is correct for Westaway's (1994a) study region: the Pearl River Mouth Basin offshore of southern China.

highly lithified metamorphic rocks forming the broad interflues between river gorges.

A fundamental difficulty with Molnar & England's (1990) view (Fig. 2) is that it ignores flow in the weak layer forming the lower continental crust. The present study will instead focus on two processes, which incorporate flow in this layer and which can each cause uplift of land surfaces in onshore areas, as well as a corresponding subsidence of the sea floor in offshore areas. The first is the isostatic response – involving flow in the weak lower crust – to increased rates of erosion (Fig. 4). The second is the isostatic response – also involving flow in the lower crust – to repeated localised cyclic loading of the Earth's surface (by ice sheets and/or fluctuations in global sea-level) (Fig. 5). Both these processes can be expected to occur to some extent in many regions (see below): they will both affect the state of isostatic equilibrium (i.e., pressure equilibrium at the base of the upper-crustal brittle layer) and thus both affect the topography. However, as will become clear below, the calculated responses to both processes can be very similar, and so separating out their individual contributions can be difficult.

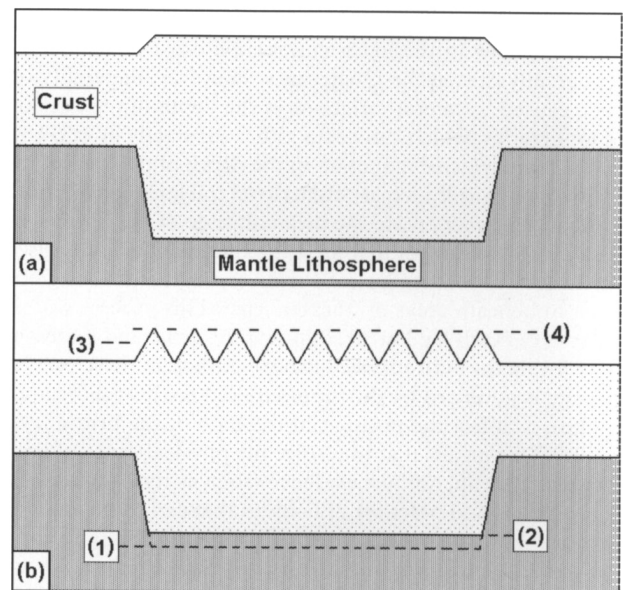


Fig. 2. The Molnar & England (1990) explanation for increasing relief in the Quaternary. Pre-existing land surfaces (a) experience increased rates of erosion resulting from the changing climate. The resulting localised incision (b) causes a small reduction in the mean thickness of the crust, resulting in upward movement of the base of the crust from (1) to (2) in accordance with conventional Airy isostasy. Fragments of the original land surface preserved on interflues uplift by an equivalent distance, from (3) to (4). Thus, although the mean altitude of the new land surface will be slightly less than that of the original land surface in (a), due to the reduction in mean crustal thickness, the altitude of the remaining fragments of the original land surface will increase. Note that this scheme ignores flow in the lower continental crust, and thus ignores the full complexity of the uplift response when continental crust is eroded (see Fig. 4 below).

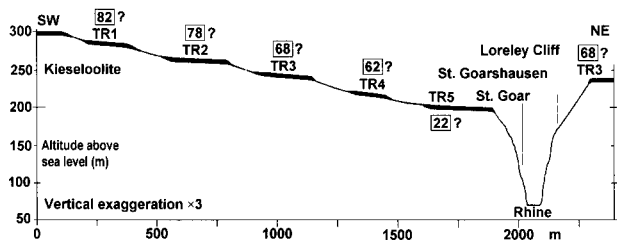


Fig. 3. Transverse profile across the Middle Rhine gorge at the famous Loreley Cliff. This Fig., adapted from part of Fig. 2 of Bibus & Semmel (1977), is modified from Westaway (2001a), Fig. 12a, to show the interpreted OIS for each river terrace. Note the transition from a broad floodplain in the Early Pleistocene, when terraces TR1 to TR5 formed, to the present much narrower cliff-lined gorge around the end of deposition of terrace TR5: a consequence of faster incision caused by an increase in the uplift rate of the adjacent land surface in the Middle Pleistocene.

Both processes depend on transient thermal disequilibrium within the continental crust, being calculated as perturbations to an assumed pre-existing steady-state regime. The time-scale over which such perturbations persist relates to the thermal time-constant of the crust, t_c , defined (Westaway, 2002b) as:

$$t_c = \frac{H^2}{\pi^2 \kappa} \quad (1)$$

where H and κ are the thickness and thermal diffusivity of the crust. The value of κ is $\sim 1.2 \times 10^{-6} \text{ m}^2 \text{ s}^{-1}$ for continental crust (e.g., Westaway, 2001a). Taking H as $\sim 30 \text{ km}$, t_c can thus be estimated as $\sim 2.4 \text{ Ma}$. Modelling studies (e.g., Westaway, 2001a, 2002b; Westaway et al., 2002) indicate that the transient response following a change in conditions becomes observable on a time scale of the order of $\sim t_c/10$ after the change. Such transient responses are thus evident on time scales of between a few hundred thousand years and a few million years after the change in conditions. This is precisely the range of time scales that is relevant to Quaternary geomorphology. As a result, it is likely that integration of geomorphological studies with physical modelling will in future provide great insights into the mechanisms governing Quaternary environmental change. As Westaway (2001a) has noted, such studies may elucidate the role of feedback mechanisms coupling climate change and crustal deformation.

The resulting development in physical modelling techniques may also have applications to wider geological problems. This is because, for reasons to do with computational complexity, hitherto commonly used techniques for modelling crustal deformation that do incorporate flow in the lower continental crust (such as King et al., 1988, and Kusznir et al., 1991) (and their many derivatives) have not considered rates of deformation. Instead, they only model

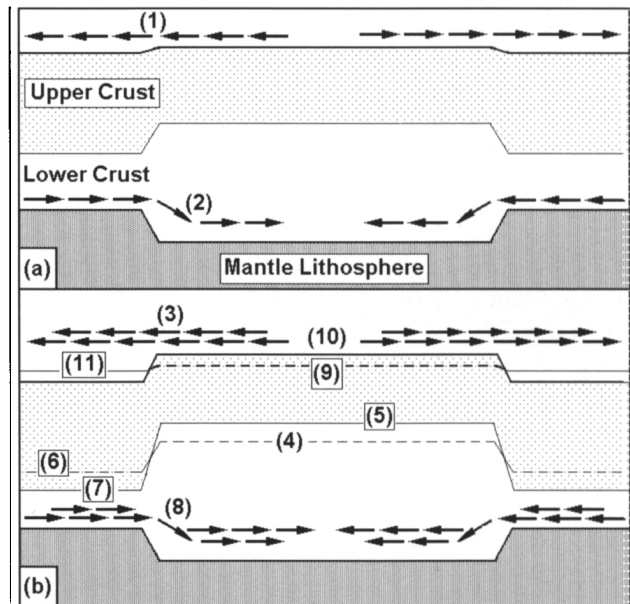


Fig. 4. Cartoons illustrating uplift induced by an increase in the rate of erosion of a land surface. In (a), a steady state situation exists in which an upland region is eroding at a uniform rate, and the eroded material is transported (1) into an adjacent depocentre. The greater depth of the base of the brittle layer beneath the depocentre than beneath the eroding sediment source establishes a pressure gradient, which drives lower crust from beneath the depocentre to beneath the sediment source (2) at the same rate as the sediment transport in the opposite direction. As a result, the eroding land surface and sediment surface in the depocentre are maintained at constant levels. In (b), the erosion rate of the upland region has increased due to a change in climate, causing a higher rate of sediment transport (3) to the depocentre. As a result, the pre-existing steady state no longer exists, and the base of the brittle layer begins to progressively advect upward relative to the eroding land surface, from (4) to (5). The increased rate of sedimentation in the depocentre causes a corresponding progressive downward advection of the base of the brittle layer beneath the depocentre, relative to the local sediment surface, from (6) to (7). As a result, the horizontal pressure gradient from beneath the depocentre to beneath the sediment source progressively increases, driving lower-crustal flow in this sense at progressively greater rates (8). Taking account of the changes in crustal conditions, and the requirement to conserve crustal volume overall, the resulting overall response will involve progressive uplift of the eroding land surface, from (9) to (10), and progressive subsidence of the sediment surface in the depocentre, which will be accompanied by an increase in bathymetry (11). Points in the land surface that are not eroding will of course uplift faster than the rate of increase in altitude of the eroding parts of the land surface, as in Fig. 2.

the overall effect of deformation of the crust from an assumed initial state to a specified final state, the deformation being assumed to occur on a time scale that is long enough for whatever lower-crustal flow that is induced to have time to occur. To be fair, age control (and hence control on rates of deformation) within the geological record is frequently poor, and one also usually has little *a priori* constraint on the viscosity at any point in the lower crust, making it dif-

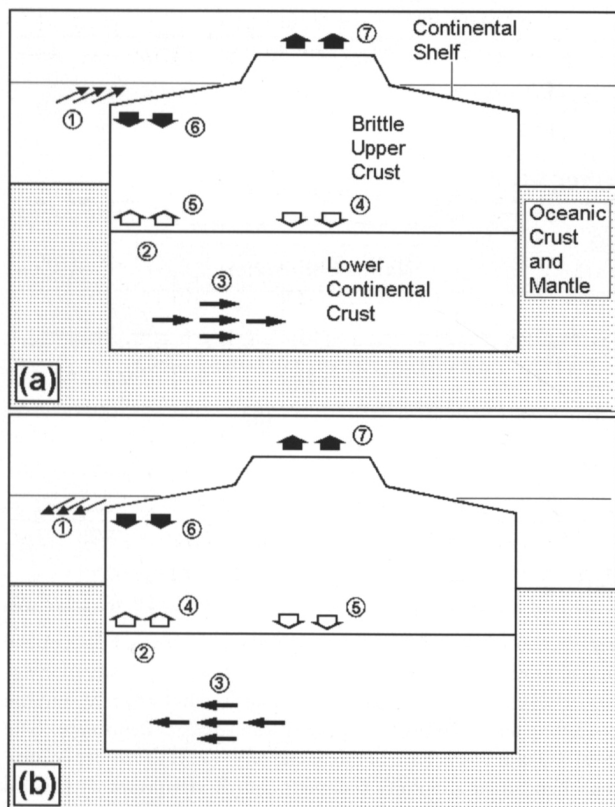


Fig. 5. Cartoons illustrating the mechanism for uplift induced by cyclic surface loading. (a) During interglacial marine highstands, the rise in sea level (1) causes an increase in the pressure at the base of the brittle layer beneath the offshore shelf (2). This causes a landward pressure gradient, which drives relatively cool lower crust from beneath the shelf to beneath the land (3). This inflow of relatively cool lower crust perturbs the geothermal gradient beneath the land, causing the base of the brittle layer to advect downward (4). The effect of earlier flow of warm lower crust to beneath the offshore shelf causes a corresponding perturbation to the offshore geothermal gradient, which causes the base of the brittle layer to advect upward (5). Taking account of the need to balance overall crustal volume within a closed system, the overall isostatic response to these processes requires the sea floor of the shelf to adjust downward, causing net thinning of the offshore crust and deepening of the shelf sea (6), and thickening of the crust beneath the land, causing the land surface to uplift (7). (b) During glacial marine lowstands, the fall in sea level (1) causes a decrease in the pressure at the base of the brittle layer beneath the offshore shelf (2). This causes a seaward pressure gradient, which drives relatively warm lower crust from beneath the land to beneath the shelf (3). This inflow of relatively warm lower crust perturbs the geothermal gradient beneath the shelf, causing the base of the brittle layer to advect upward (4). The effect of earlier flow of cool lower crust to beneath the land causes a corresponding perturbation to the onshore geothermal gradient, which causes the base of the brittle layer to advect downward (5). Taking account of the need to balance overall crustal volume within a closed system, the overall isostatic response to these processes requires the sea floor of the shelf to adjust downward, causing net thinning of the offshore crust and deepening of the shelf sea (6), and thickening of the crust beneath the land, causing the land surface to uplift (7). If, in reality, material is gained or lost from a given section line, due to components of flow perpendicular to the section, the resulting uplift response will have the same form, but a different amplitude, to that calculated for the ideal case assuming conservation of volume.

difficult to establish how fast it can flow. By not considering rates, these established techniques effectively allow these two problems to be traded off against each other, making it possible to say something quantitative about crustal deformation within the geological record without making too many untestable assumptions. In contrast, the modelling of detailed geomorphological records – of river and marine terrace sequences – that span much of the Quaternary provides control on rates of deformation and thus – as, for instance, Westaway et al. (2002) and Westaway (2002b) have shown – on the viscosity of the lower continental crust in each study locality. One may thus anticipate that future studies on the same lines will gradually establish likely values for the lower-crustal viscosity in different geological settings, which will then be usable in modelling other aspects of crustal deformation. Thus, geomorphology, long neglected by the geological community as of little relevance to the fundamentals of geology, may well provide the key to the future more rigorous understanding of many geological problems.

In recent years, the view has gained ground within the geomorphological community that the formation of long-term river terrace staircases requires uplift of the land surface on which each terrace sequence develops (e.g., Van den Berg, 1996; Maddy, 1997; Van den Berg & Van Hoof, 2001). Reviews of river terrace data sets (e.g., Westaway, 2001a, 2002a) indicate that in many localities the uplift rate increased around the end of the Early Pleistocene (at or shortly after oxygen isotope stage 22 (OIS 22)). In some localities this transition is very marked: for instance, along the Middle Rhine in western Germany, a minimal uplift rate in the late Early Pleistocene gave way to quite rapid uplift, at $>0.2 \text{ mm a}^{-1}$, as the river switched from aggrading across a broad valley with low relief to incising its modern steep-sided gorge (Westaway, 2001) (Fig. 3). In south-east England, the Lower Thames flowed across a region that was subsiding in the Early Pleistocene but began uplifting at rates of up to $\sim 0.09 \text{ mm a}^{-1}$ in the Middle Pleistocene (e.g., Bridgland & Allen, 1996; Westaway et al., 2002). River terrace sequences that date from the Late Pliocene or earlier, notably of the Maas in the south-eastern Netherlands (e.g., Van den Berg, 1996; Van den Berg & Van Hoof, 2001; Westaway, 2001), also preserve evidence of an earlier increase in uplift rates, around 3 Ma. The uplift rate subsequently tailed off before the second rate increase around 0.9 Ma. The striking similarities between many long-term river terrace sequences (e.g., Westaway, 2002a) suggests that a common set of causal mechanisms is involved, and as many of these sequences occur in areas where active faulting in the

brittle upper crust is unknown, the required surface uplift can only plausibly result from coupling between surface processes and lower-crustal flow. As Westaway (2001a, 2002b) and Westaway et al. (2002) have noted, the resulting uplift rates can contribute to constraining the viscosity of the lower continental crust.

Unfortunately, my recent experience indicates that this potential significance of geomorphological datasets for constraining crustal rheology is not widely appreciated within the geomorphological community. The present manuscript will therefore work through and justify each of the assumptions behind the modelling methods in Figs 4 and 5. I note in passing that deformation of the brittle upper crust caused by lower-crustal flow should be referred to as atectonic deformation (e.g., Kaufman & Royden, 1994) to distinguish it from tectonic deformation that is caused by plate motions. If one does not yet know what is causing the crustal deformation at a given locality, then it should be described simply as 'crustal deformation': due to its potential ambiguity the colloquial term 'tectonics' should ideally not be used.

Modelling assumptions

The modelling techniques summarised in Figs 4 and 5 are based on several physical assumptions. I will now summarise the evidence from which each of these assumptions follows. The assumptions are, first, that in regions of normal crustal thickness and heat flow, the continental crust consists of an upper, brittle layer, and a lower layer, which deforms by flow. The base of the brittle layer is a thermal boundary, not a compositional boundary. Second, lateral variations in the pressure at the base of the brittle layer, caused by the weight of the overlying rock layer (plus the water load in submerged regions, or the ice load in glaciated regions), establish horizontal pressure gradients that drive flow in the lower crust. Third, the brittle upper crust is able to flex as well as deforming by faulting. Its flexural rigidity is low, such that flexural bending stresses are small and do not significantly influence the resulting crustal configuration, which is determined instead by inflow or outflow of lower crust at depth. In contrast, the mantle lithosphere beneath the crust can range in thickness from a few tens of kilometres to more than 100 km. Depending on its thickness, it may either flex readily (as is assumed for the brittle upper crust) or remain essentially rigid on the horizontal scale of the overlying crustal deformation. Calculations of the isostatic response of the lithosphere should thus take account of the spatial scale required for flexure of the mantle lithosphere. Finally, the viscosity at each point in the crust is determined

by the local temperature. The rheology is assumed to be linear, with viscosity not dependent on strain rate over the range of strain rate relevant to geological processes.

Nature of the base of the brittle layer

It is well known that, in most regions of continental crust, seismicity is confined to the upper part of the crust, and crustal levels deeper than $\sim 15 \pm 5$ km are aseismic. The continental crust thus usually consists of an upper, brittle layer, overlying a plastic layer that behaves like a viscous fluid over geological time scales. It was established many years ago, on the basis of observational studies involving accurate location of earthquakes and rheological and thermal modelling, that the boundary between these layers is thermal – not compositional – being the depth at which the temperature is $\sim 350^\circ\text{C}$ (e.g., Sibson, 1982; Kuszniir & Park, 1984).

Existence and role of lateral pressure gradients

The assumption that the vertical stress within the upper-crustal brittle layer equals the lithostatic pressure (plus any hydrostatic pressure) is standard in rock mechanics (e.g., Turcotte & Schubert, 1982, p. 354). Like any other confined fluid, the lower crust will flow in response to lateral variations in confining pressure, which result from lateral variations in depth of the base of the overlying brittle layer.

A key feature of the models in Figs 4 and 5 is that, in the computer programs used to implement them, the base of the brittle layer is not regarded as fixed, but is instead recalculated for each time step of each model run. This is because, in Fig. 5, the lower crust that flows to beneath a region will have a different temperature from the material that is already there. The presence of this inflow of material will thus affect the geothermal gradient within the crust, which will perturb the depth of the base of the brittle layer. In Fig. 4, erosion and sedimentation will also affect the depth of the base of the brittle layer. The onset of erosion will cause the base of the brittle layer to advect upward relative to the series of instantaneous positions of the Earth's surface. This will reduce the pressure at the base of the brittle layer below the value expected in the absence of erosion. Conversely, the 'thermal blanketing' effect following the onset of sedimentation will cause the base of the brittle layer to advect downward relative to the series of instantaneous positions of the upper surface of the sediment. This will increase the pressure at the base of the brittle layer above the value expected in the absence of

sedimentation. As a result, a pressure gradient will become established in the lower crust from beneath the depocentre to beneath the eroding sediment source, which will act to drive lower crust in this direction.

This ability of recent models to dynamically recalculate the position of the base of the brittle layer in response to surface processes represents a major improvement over earlier solutions, such as those by King et al. (1988), King & Ellis (1990), and other examples discussed by Mitchell & Westaway (1999), which treated the base of the brittle layer as fixed relative to the surrounding rock column irrespective of what surface processes were assumed to be occurring. Consequences of this omission are analysed by Mitchell & Westaway (1999) and Westaway (2002b). These consequences are not repeated in detail here, other than to note that they can be drastic. Failure to dynamically recalculate the position of the base of the brittle layer has indeed resulted in publications claiming that the expected sense of lower-crustal flow is outward from beneath eroding mountain ranges and/or inward to beneath depocentres: the opposite to what is determined when the calculations incorporate this effect (Figs 1, 4).

In the recent literature, Westaway (1994a) reported the first study to suggest that eroding sediment sources and depocentres within the continental crust may typically be coupled by sediment transport and lower-crustal flow as shown in Fig. 1. Although this was thought at the time to be an original idea, it turns out to be equivalent in principle to a scheme proposed by Herschel (1837) (Fig. 6) (see below). Theoretical analyses (e.g., Stüwe et al., 1994; Mitchell & Westaway, 1999; Westaway, 2002b) suggest that it is

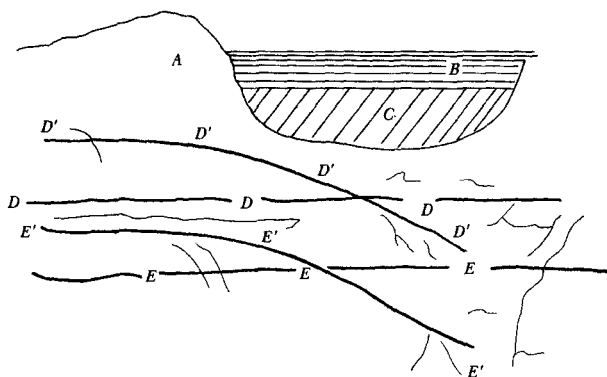


Fig. 6. Sir John Herschel's 1834 view of the uplift of Scandinavia driven by sediment loading in the Baltic Sea. A is Scandinavia; B, the Baltic Sea; C, recently deposited sediments in the Baltic Sea; D, a marker level within the upper crust; and, E, the semi-fluid rock beneath. The weight of the recent sediments (C) depresses the seabed (D) to D' and thus displaces the semi-fluid rock (E) to E', which uplifts the shoreline of Scandinavia (A) and renews the erosion gradient. From Greene (1982, p. 108); based on a drawing from Herschel (1837).

possible to establish a steady-state situation where erosion and sedimentation are maintained at constant rates for long enough that the base of the brittle layer is held at a constant depth beneath the eroding land surface, and a constant (but greater) depth beneath the sediment surface in the depocentre. The sediment transport at the Earth's surface between the eroding sediment source and the depocentre is thus balanced by an equivalent rate of lower-crustal flow, such that a constant crustal thickness is maintained beneath both the sediment source and the depocentre (counting the layer of sediment as part of the crustal thickness and neglecting any difference in density between compacted sediment and crustal basement).

In this steady-state situation, rock at depth beneath the sediment source will uplift towards the series of instantaneous positions of the Earth's surface, before being removed by erosion on reaching this surface. However, although rock at depth is uplifting, the Earth's surface itself maintains a constant altitude (because the process is assumed to be isostatically compensated and the crustal thickness remains constant). When describing such a situation it is thus vital to be clear about what one means by 'uplift': one must in general distinguish between uplift of rocks towards an eroding land surface (which may or may not be at a constant altitude) and uplift of a land surface (which may or may not be eroding) relative to a fixed datum such as the envelope of successive global sea-level maxima during major Quaternary interglacials. Although previous appeals have been made within the literature to maintain such clarity (e.g., by England & Molnar, 1990), it is not always regarded as a priority (c.f., Smith et al., 1999).

Under non-steady-state conditions, for time $\leq t_c$ after the start of erosion (or a change in erosion rates), the situation is more complex, as is discussed by Westaway (2002b) following the development of relevant quantitative theory. After an increase in erosion rate, the base of the brittle layer will become shallower at a rate that is proportional to the change in erosion rate. This will set up an inward pressure gradient – of magnitude increasing with time – to beneath the eroding region, which as time progresses will drive increasingly vigorous lower-crustal flow to beneath this region. The expected result will be an increase in crustal thickness, and thus in the mean altitude of the land surface. Such an increase in mean altitude of the land surface will be expected to result in increased topographic gradients at the margins of the eroding region, which may cause further increases in rates of erosion, which may in turn increase the rate of increase in altitude of the Earth's surface. This combination of positive feedback mechanisms may explain

the presence of mountain ranges in regions of negligible present-day plate convergence, such as the Sierra Nevada, Appalachians, Pyrenees, Betics, Atlas, Carpathians, Greater Caucasus, Urals, and other mountain ranges in central Asia. Although most of these modern mountain ranges are in regions that accommodated ancient plate convergence, the persistence of their topography (and, above all, the evidence available in most cases for Quaternary increases in mean surface altitude) favours the involvement of coupling between surface processes and lower-crustal flow in their development (Fig. 4). Mitchell & Westaway (1999) indeed presented a first-order analysis of the Greater Caucasus from this point of view.

As Westaway (2001a) and Westaway et al. (2002) also point out, the mechanism in Fig. 5, involving lower-crustal flow induced by cyclic surface loading, can also enhance topographic relief, even in the absence of erosion. Cyclic loads caused by ice sheets or by fluctuations in global sea-level will induce cyclic pressure gradients in the lower crust. At first sight it appears that whatever flow occurs when any load is applied will be reversed when the load is subsequently removed. However, Westaway (2001a) and Westaway et al. (2002) have shown that this is not so: crust flowing from beneath the offshore shelf to beneath the land, driven by water loading during interglacial marine highstands, is expected to be cooler than the crust already present beneath the land. This is because lower-crustal flow is expected to be fastest at levels roughly nine tenths of the way between the base of the brittle layer and the Moho (see Westaway, 1998, also Fig. 7), and the temperature of the crust at this level will vary with the local Moho temperature. Other factors (such as radioactive heating in the upper crust, and mantle lithosphere thickness) being equal, the Moho temperature will vary with crustal thickness: it will thus be lower beneath offshore areas, where the crust is thinner, than beneath onshore areas. Likewise, crust flowing offshore at times of reduced water loading will warm the crust already there. Westaway (2001a) and Westaway et al. (2002) have showed that the overall effect of many cycles of lower-crustal flow induced in this manner will be to affect the depth at the base of the brittle layer so as to cause net thickening of the crust that is originally warmer, and thinning of the crust that is initially cooler. The resulting isostatic response involves uplift of the land surface in areas where the crust is initially warmer and subsidence where it is initially cooler. The fluctuating climate in the Quaternary can thus have brought about the observed changes in landscape development even beyond the regions affected by glaciation.

Flexural rigidity of the upper crust and mantle lithosphere

In recent years there has been a divergence of views between the Earth Sciences and geomorphological literatures as to what is an appropriate order-of-magnitude value for the flexural rigidity of the upper-crustal brittle layer in continental crust with typical thickness and heat flow. The flexural rigidity D of an elastic layer of thickness H , Young's modulus E , and Poisson's ratio ν is defined as

$$D = \frac{E H^3}{12(1-\nu^2)} \quad (2)$$

(e.g., Turcotte & Schubert, 1982, p. 115). The flexural rigidity governs the spatial scale over which curvature can develop within an elastic layer, the natural wavelength λ for flexure of an elastic layer of crust with density ρ_c ($\sim 2700 \text{ kg m}^{-3}$) being given by

$$\lambda = 2 \pi (D / \rho_c g)^{1/4} \quad (3)$$

where g ($\sim 9.81 \text{ m s}^{-2}$) is the acceleration due to gravity (e.g., Turcotte & Schubert, 1982, p. 123). The abundant geological evidence of structures affecting basement within the brittle layer with substantial curvature over scales of 10 km or less unequivocally requires a low flexural rigidity: in many cases as low as $\sim 10^{19} \text{ N m}$ (e.g., Buck, 1988). It was also noted many years ago (e.g., by King et al., 1988) that if one takes the expected typical values for E , H and ν of $\sim 80 \text{ GPa}$, $\sim 15 \text{ km}$, and ~ 0.25 , and substitutes them into equation (2), one predicts a much higher flexural rigidity for the brittle layer, of $\sim 10^{22} \text{ N m}$, instead, for which λ (from equation (3)) is as high as $\sim 200 \text{ km}$. Another way of expressing this discrepancy is to determine an 'effective elastic thickness' for the brittle layer, H_e , by rearranging equation (2) as

$$H_e = \sqrt[3]{\left(\frac{12 D (1-\nu^2)}{E}\right)} \quad (4)$$

Many geological structures indeed indicate H_e values as low as $\sim 1\text{--}3 \text{ km}$ (e.g., King et al., 1988; King & Ellis, 1990; Kusznir et al., 1991; Westaway, 1992a; Armijo et al., 1996). For the past decade or so, effort has thus been focussed on trying to understand the discrepancy between these observed and expected values for flexural rigidity and effective elastic thickness of the brittle upper crust.

One suggestion, by Kusznir et al. (1991), was that warping of the brittle layer causes much of its thickness to fracture, making it unable to support elastic stress and thus concentrating this stress in a thin 'fibre' at depth. In this scheme, values of H_e determined from equation (4) represent estimates of the actual thickness of this fibre. This scheme predicts that, in

the early stages of crustal deformation when structural curvature is gentle, the flexural rigidity of the brittle layer is high: but it later gradually reduces with continued deformation. However, Westaway (1992a) noted some apparent counter-examples to this view, and suggested an alternative interpretation, in which the Young's modulus E decreases on long time scales from its short-term value of ~ 80 GPa (estimated from the velocities of seismic waves) to a long-term value that is $\sim 1/100$ to $\sim 1/1000$ of this value – ~ 80 – 800 MPa – due to the effects of slow anelastic processes such as pressure solution creep, regardless of the amount of pre-existing deformation. Later studies such as Armiño et al. (1996) have also favoured this view.

In contrast, in the geomorphological literature, many studies have been published in which the warping of the crust across passive continental margins, on scales of many hundreds of kilometres between offshore depocentres and eroding subaerial land surfaces, is modelled as a flexural isostatic effect (e.g., Gilchrist & Summerfield, 1990; Kooi et al., 1991; Kooi & Beaumont, 1994; Gilchrist et al., 1994; Pazzaglia & Gardner, 1994). To account for the very gentle structural curvature typically observed in these situations requires such models to incorporate a very high flexural rigidity. For instance, Kooi & Beaumont (1994) considered models with the elastic thickness of the brittle layer set as high as 30 km, making the assumed flexural rigidity in excess of $\sim 10^{23}$ N m. However, there is no justification whatsoever for setting the elastic thickness in excess of the actual thickness of the brittle layer. As a result such high flexural rigidities have no physical basis in regions of normal crustal thickness and geothermal gradient.

Another possibility is, of course, that the characteristic very gentle warping of the continental crust across passive margins may have nothing to do with flexural isostatic compensation of elastic stresses over scales of hundreds of kilometres. As already noted, the present study indeed adopts a different approach, in which isostatic equilibrium is determined by calculating the flow response within the lower crust to pressure gradients that develop as a result of lateral variations in the pressure (and, hence, depth) of the base of the brittle layer. This isostatic response is thus calculated for each locality on a pointwise basis, and flexural stresses are neglected. The justification for neglecting these stresses is that the flexural rigidity of the brittle layer is low (for reasons already discussed) and so the lateral variations in uplift that are being modelled result in such gentle warping of the brittle layer that the associated bending stresses are small.

The base of the mantle lithosphere, like the base of the brittle upper crust, is a thermal boundary, being

determined by the temperature threshold of ~ 1400 °C that marks the transition to the convecting part of the mantle (the asthenosphere). The Moho is of course a compositional boundary, but its temperature is typically ~ 600 °C in continental crust of normal thickness and geothermal gradient. Due to the lack of radioactive heat production in the mantle lithosphere, unlike in the continental crust, the geothermal gradient across the mantle lithosphere is typically much lower than in the crust. The temperature increase from ~ 600 °C to ~ 1400 °C thus typically occurs across a much greater depth range than that from ~ 0 °C to ~ 600 °C. As a result, the mantle lithosphere is frequently ~ 100 km thick beneath continental crust of normal thickness and geothermal gradient. From equation (4), the flexural rigidity of the mantle lithosphere is likely to be $\sim 10^{25}$ N m, making its natural wavelength for flexure (estimated using equation (3) with an appropriate density of ~ 3300 kg m⁻³ instead of the crustal density) ~ 800 km. As many uplifting regions have dimensions smaller than 800 km, it is likely that whatever crustal thickness changes have developed due to lower-crustal flow beneath these regions are largely uncompensated by deflection of the mantle lithosphere. In such a situation, the growth in topography due to inward lower-crustal flow to beneath a region will NOT be accompanied by the development of a lower-crustal 'root', making it unlike the conventional Airy isostatic response to crustal thickening. However, in some regions (such as the Rhenish Massif analysed by Westaway (2001), with dimensions of ~ 200 km) the high heat flow makes the mantle lithosphere unusually thin – no more than a few tens of kilometres thick. As a result, it may be able to flex on the scale of the observed crustal thickening, leading to the development of a lower-crustal root in a manner that approximates conventional Airy isostasy.

Choice of rheology for the lower continental crust

The major difficulty in any quantitative analysis of lower crustal flow is the choice of rheology. One needs to establish what the lower crust is made of and then select a rheological law for that material under the appropriate conditions of temperature and strain rate. For practical reasons, it has been difficult to run laboratory rock mechanics experiments at strain rates of $< 10^{-7}$ s⁻¹. At such high strain rates, higher temperatures than are usual within the continental crust are needed for levels of applied differential stress $\Delta\sigma$ to be ~ 1 GPa or less, within the range of measurement using standard apparatus. The rheology of quartz and other minerals at geological strain rates of $\sim 10^{-15}$ s⁻¹ or less and at crustal temperatures of ~ 600 °C or less

is thus not directly measurable in the laboratory, where experiments are run at strain rates many orders-of-magnitude greater than geological processes and at much higher temperatures than can be expected in crust of normal thickness. One therefore needs to extrapolate from their results over a wide range of parameter values.

In my opinion the most appropriate starting assumption of a simple material to use as a laboratory analogue for the lower continental crust is polycrystalline quartzite. This is because, although quartzite is unlikely to form the bulk of the lower crust by volume, it is the weakest material likely to be present. Grains of quartzite can thus deform to allow grains of stronger materials to 'flow' past them.

Laboratory measurements of rock rheology at a given absolute temperature T typically yield results that can fit power laws between corresponding elements of the stress and strain rate tensors such as σ_{xz} and E_{xz} of the form

$$E_{xz} = A \sigma_{xz}^n \quad (5)$$

where A and n are empirical constants and $n > 1$. The resulting viscosity $\eta = \sigma_{xz} / E_{xz}$ is thus expressed as

$$\eta = A^{-1/n} E_{xz}^{1/n-1} \quad (6)$$

However, this requires $\eta \rightarrow \infty$ as $E_{xz} \rightarrow 0$, which is physically unrealistic. At some lower bound to strain rate (5) thus breaks down. If at even lower strain rates n were less than 1, η would tend to zero as $E_{xz} \rightarrow 0$, which would conflict with abundant evidence (e.g., the propagation of seismic S-waves) that requires finite viscosities in the lower continental crust. The only condition that makes physical sense is thus for $n=1$ in the limit of $E_{xz} \rightarrow 0$. This point has long been accepted in fields making widespread use of empirical measurements of rheology, such as Materials Science (e.g., Chermisinoff, 1993, p. 12). Many texts indeed highlight the need to avoid misuse of power law rheologies by extrapolating them outside the limited range of stress or strain rate where measurements were made (e.g., Whorlow, 1992, p. 15). However, Earth Scientists have instead routinely extrapolated empirical power laws to arbitrarily small strain rates, and have argued on the basis of such extrapolations that the lower crust has a very high viscosity in crust of normal thickness and geological gradient. It is thus important to establish whether the breakdown of power law behaviour with $n > 1$, determined from laboratory measurements, is or is not above the upper bound to geological strain rates of $\sim 10^{-15} \text{ s}^{-1}$.

Several empirical or semi-empirical flow laws combine power-law behaviour at moderate strain rates with linear behaviour at low strain rates. A widely

used example, by Cross (1966), can be written in the form

$$\eta = \eta_{\infty} + \frac{\eta_0 - \eta_{\infty}}{1 + (E_{xz} / E_{xz,c})^N} \quad (7)$$

The parameters η_0 and η_{∞} are the viscosities at zero and infinite strain rates; $E_{xz,c}$ being the critical shear strain rate at which η is the mean of these limiting values. This transition between these limiting values can be related to changes in ordering behaviour: at very low strain rates, polycrystalline aggregates have a random structure, whereas at high strain rates their fabric becomes ordered parallel to the flow.

Westaway (1998) made the first attempt to fit a law of this form to rock mechanics data representing the lower continental crust. He proposed that the power-law behaviour observed in the laboratory marks the transition between limiting viscosities, but geological conditions lie within the low strain rate limiting regime. Westaway (1998) thus represented the temperature dependence of the low strain rate limit of viscosity, $\eta_0(T) = \eta(T, E_{xz} \rightarrow 0)$, as

$$\eta_0(T) = \eta_L \exp(G / RT), \quad (8)$$

where G is the molar activation energy of the microstructural process that causes the temperature-dependence of viscosity (for which Westaway (1998) adopted a preferred value of 200 kJ mol^{-1}), R is the molar gas constant ($8.3143 \text{ J K}^{-1} \text{ mol}^{-1}$), and η_L is a temperature-independent material property of wet or dry quartzite, also assumed independent of pressure, which Westaway (1998) estimated as 200 kPa s . Using (8), the viscosity of quartzite can be calculated at temperatures appropriate for the lower continental crust: with $G=200 \text{ kJ mol}^{-1}$: it is $7.4 \times 10^{21} \text{ Pa s}$ at 350°C ; $6.5 \times 10^{18} \text{ Pa s}$ at 500°C ; and $4.2 \times 10^{16} \text{ Pa s}$ at 650°C .

Like other studies (e.g., Luan & Paterson, 1992), Westaway's (1998) analysis precludes G significantly higher than $\sim 200 \text{ kJ mol}^{-1}$, but could permit lower values, down to $\sim 100 \text{ kJ mol}^{-1}$. Lower values of G would result in lower predicted viscosities across the temperature range for the lower continental crust. However, a major aim in deriving these lower-crustal viscosity solutions is to enable feasibility tests of models involving lower-crustal flow, as in the studies by Westaway (2001a) and Westaway et al. (2002): by showing that a given rate of lower-crustal flow, required for a model to work, is compatible with what is known about the crustal temperature in the study region. To make these tests as rigorous as possible, they have been carried out using the viscosities that follow from assuming $G=200 \text{ kJ mol}^{-1}$. Such tests would indeed become much less stringent if the lower viscosities that would

follow from assuming smaller values of G were used instead.

Westaway (1998) also determined an approximate solution for the profile of horizontal velocity within lower crust with a uniform geothermal gradient subject to the assumption that viscosity is independent of strain rate (i.e., the rheology is linear) with viscosity varying with temperature according to equation (8). Examples of the form of the solution obtained are shown in Fig. 7. This velocity field differs somewhat from the ideal parabolic profile for channel flow in an isoviscous fluid (thin line in Fig. 7). The main difference is that it is skewed, with the peak velocity roughly nine tenths down through the channel, compared with halfway down for the isoviscous case. A second difference is that in the lower crust with temperature-dependent viscosity the flow is quite strongly concentrated near the depth corresponding to peak velocity. The sharpness of this peak increases with molar activation energy and geothermal gradient: as is illustrated in Fig. 7, with $G=200 \text{ kJ mol}^{-1}$, this peak is sharper with the higher geothermal gradient in Fig. 7(a), where almost all the flow is in the lower half of the lower crust, than for the lower geothermal gradient in

Fig. 7(b). Note also the much slower flow in the cold lower crust in Fig. 7(b) than in the hotter lower crust in Fig. 7(a), even though the pressure gradient in (b) is greater. With the same pressure gradient, the flow would be about 140 times faster in (a) than in (b).

One may define the effective viscosity η_e of the lower crust as the viscosity of an isoviscous layer for which the horizontal flux of material, or mean horizontal velocity, is the same as for a layer with temperature-dependent viscosity (see also Fig. 7 caption). Westaway (1998) estimated that, as a rough 'rule of thumb', if G is assumed to be 200 kJ mol^{-1} , the effective viscosity of the lower crust can be estimated as roughly sixty times the Moho viscosity η_m . The precise ratio of these viscosities depends on the lower-crustal thickness and geothermal gradient: for the configuration in Fig. 7(a), where the lower crust is 20 km thick, with a geothermal gradient of 15°C km^{-1} resulting in a Moho temperature of 650°C , η_m is $\sim 4 \times 10^{16} \text{ Pa s}$ and η_e is $\sim 3 \times 10^{18} \text{ Pa s}$, a ratio of ~ 70 . For the case in Fig. 7(b), where the lower crust is 15 km thick but with a lower geothermal gradient of 10°C km^{-1} , making the Moho temperature 500°C , η_m would be $\sim 7 \times 10^{18} \text{ Pa s}$ and η_e would be $\sim 2 \times 10^{20} \text{ Pa s}$, a ratio of ~ 25 .

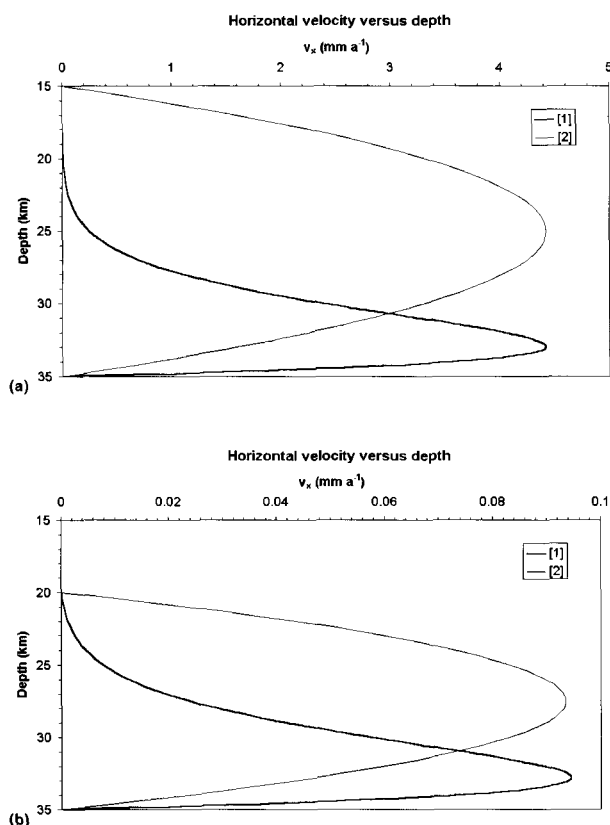


Fig. 7. Profiles of steady-state flow in hot (a) and cooler (b) lower continental crust. Thick lines [1] illustrate the depth-dependence of velocity in lower-crust with temperature-dependent viscosity and a uniform geothermal gradient. Thin lines [2] illustrate, for comparison, the very different parabolic velocity profile for isoviscous

lower crust. Calculations for lines [1] use an approximate analytic solution obtained by Westaway (1998), with the vertical variations in viscosity calculated using equation (8) with $G=200 \text{ kJ mol}^{-1}$ and $\eta_L=200 \text{ kPa s}^{-1}$. (a) Line [1], adapted from Westaway (1998, Fig. 4(b)), is for a horizontal pressure gradient of $10/3 \text{ Pa m}^{-1}$ across a 20-km-thick lower crustal channel with a geothermal gradient of 15°C km^{-1} : with temperatures of 350°C at the 15 km deep base of the brittle layer and 650°C at the 35 km deep Moho, where the calculated viscosity is $4.16 \times 10^{16} \text{ Pa s}$. Line [2] is calculated for the same pressure gradient with a viscosity of $1.13 \times 10^{18} \text{ Pa s}$, chosen to give the same peak velocity as for line [1]. On line [1], this peak occurs at 33 km depth, which is nine tenths of the way from the base of the brittle layer to the Moho. If one wished instead to scale line [2] to give the same volume flux as line [1] (i.e., to enclose the same area as between line [1] and the vertical axis) one would need to specify a viscosity of $2.95 \times 10^{18} \text{ Pa s}$, which is thus the 'effective viscosity' for the flow profile given by line [1] (see main text). See Westaway (1998) for more detail on these calculations. (b) Curve [1] is for a horizontal pressure gradient of 10 Pa m^{-1} across a 15-km-thick lower crustal channel with a geothermal gradient of 10°C km^{-1} : with temperatures of 350°C at the 20 km deep base of the brittle layer and 550°C at the 35 km deep Moho, where the calculated viscosity is $6.54 \times 10^{18} \text{ Pa s}$. Line [2] is calculated for the same pressure gradient with a viscosity of $9.02 \times 10^{19} \text{ Pa s}$, chosen to give the same peak velocity as for line [1]. On line [1], for which the effective viscosity is $1.63 \times 10^{20} \text{ Pa s}$, this peak occurs at 32.9 km depth, which is $\sim 86\%$ of the way from the base of the brittle layer to the Moho. Note that the ratio of effective viscosity to Moho viscosity is ~ 70 in (a) but only ~ 25 in (b). The constants D_1 and D_2 , required to match the boundary conditions for zero velocity at the margins of the lower-crustal channel in equation (B19) of Westaway (1998), take values of 1.02556 s^{-1} and $-0.00009 \text{ mm a}^{-1}$ in (a) and 3.86527 s^{-1} and $-0.00006 \text{ mm a}^{-1}$ in (b). See Westaway (1998) for more detail on these calculations.

Discussion

As Westaway (1994b) previously noted, Herschel's (1837) ideas (Fig. 6) about the role of lower-crustal flow in the growth of topography (summarised by Greene, 1982) warrant comparison with modern ideas. Herschel was well aware that temperature measurements in mines indicate a geothermal gradient of tens of °C per kilometre, and extrapolated this to suggest that at depths greater than a few kilometres rock is able to flow. He thus proposed that sediment loading would increase the pressure acting on this 'semi-fluid' rock, forcing it laterally away from beneath a depocentre to beneath its surroundings. As is summarised in Fig. 6, Herschel (1837) suggested that such flow, driven by sedimentation in the Baltic Sea, could explain the uplift of Scandinavia. This is of course wrong: this uplift is now well known to be the result of glacio-isostatic rebound, an idea first suggested in 1862. However, he was well aware of marine terrace sequences in many other regions, which he argued indicate uplift that could also be explained by the process in Fig. 6: he indeed thought he had found a general explanation for vertical crustal motions.

Although Herschel's (1837) views remained influential for decades, they were disregarded by geologists with field experience of mountain ranges, notably the Alps. Herschel's (1837) scheme predicts that mountain ranges should be oriented parallel to coastlines. Although many do have this geometry, it was felt by Alpine geologists that a supposedly general theory that could not explain the overall geometry of what was then the best-studied mountain range, let alone its internal structure that was already well-documented, cannot have great value. Herschel (1837) of course did not consider crustal shortening (let alone, subduction) as a cause of crustal thickening in mountain ranges, and was also unaware of the fundamental rheological difference between continental and oceanic crust: he thus pushed his ideas too far.

Nonetheless, it is worth noting that the idea that the topography of the Alps may relate to the isostatic response to inward lower-crustal flow, may – after all – have some merit. It is clear that the structure of the Alps is the result of prolonged crustal deformation caused by plate motions, including effects of southward subduction beneath Italy of an ocean attached to the Eurasian plate, and large-scale shortening of the continental crust taken up by thrust faulting. However, De Sitter (1952) first suggested that the development of topography in the Alps is unrelated to the structure: he estimated that between 1 and 2 km of uplift has occurred since the start of the Pliocene, and it is clear from his wording that he meant region-

al uplift and not local relief between mountain summits and adjacent valleys (q.v. Fig. 2). Furthermore, it is now known that rates of plate convergence across the Alps are negligible (e.g., Westaway, 1990, 1992b). In addition, localities in the northern foreland of the Alps, such as the vicinity of Vienna which has been unaffected by crustal shortening, have nonetheless experienced ~400 m of uplift since the Late Miocene, revealed by the altitudes of Late Miocene marine sediments and younger river terrace deposits of the Danube and its tributaries (e.g., Sibrava, 1972). It thus follows that the Alps themselves have uplifted farther, on this time scale, and the mechanism may well also be unrelated to crustal shortening. However, resolving the individual contributions of the processes in Figs 4 and 5 on the uplift history of the Alps is beyond the scope of this study.

Since both cyclic surface loading (Fig. 5) and non-steady-state erosion (Fig. 4) can cause surface uplift, it is important to consider in general whether the two can be distinguished observationally if a region's uplift history is known (from, say, altitudes of preserved river terraces). However, Fig. 8 suggests that making this distinction can be expected to be very difficult, due to the similarity in uplift histories predicted for both processes. In Fig. 8, the solid line [1] shows the uplift history of a non-eroding land surface as a result of cyclic surface loading starting at 1.2 Ma, supplemented by additional forcing starting at 0.9 Ma. Such a history is plausible, given that the build-up in ice volume during glacial maxima began to increase around OIS 36 (~1.2 Ma) and reached the scale of the largest Middle and Late Pleistocene glaciations in OIS 22 (~0.9 Ma) (e.g., Shackleton et al., 1990). The dashed line [2] shows a possible uplift history (of non-eroding markers such as river terraces) that results from a region undergoing a transition at 0.9 Ma from being a depocentre with a sedimentation rate of 0.1 mm a⁻¹ to eroding at a rate of 0.2 mm a⁻¹. For time since 0.9 Ma, the two histories are so similar that it is doubtful whether any observational record left from this time scale could resolve them. If, instead, remnants are preserved of dateable sediment deposited before 0.9 Ma, then one could argue that the region was previously a depocentre, thus providing a justification for adopting model [2] instead of [1]. However, if no evidence of regional cover by Early Pleistocene sediment is preserved, and no Early Pleistocene river terraces exist that would provide evidence of a pre-existing subaerial landscape with no regional sediment cover, then one may well have no clear basis for a choice of model.

My experience indicates that it can be relatively difficult to identify regions where overwhelming grounds

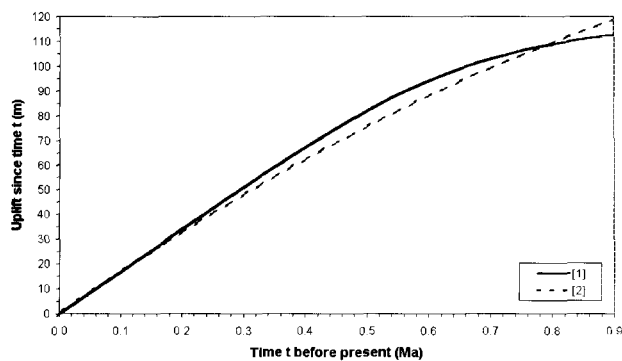


Fig. 8. Comparison of predicted uplift histories resulting from cyclic surface loading (solid line, [1]) and from non-steady-state erosion (dashed line, [2]). Solid line [1] is calculated using theory for cyclic surface loading from Westaway (2001a) and Westaway et al. (2002). Crust is assumed to be 30 km thick, with a density of 2700 kg m^{-3} and a thermal diffusivity of $1.2 \times 10^{-6} \text{ m}^2 \text{ s}^{-1}$. The base of the brittle layer is assumed initially at 15 km depth, with lower-crustal flow is concentrated nine-tenths of the way between this depth and the Moho, at 28.5 km depth. The assumed geothermal gradient in the lower crust is $10 \text{ }^\circ\text{C km}^{-1}$. The adjacent subsiding region which is assumed to supply the lower-crust that sustains the calculated uplift is loaded by water with a density of 1000 kg m^{-3} . The dimensions of, and temperature contrast between, these uplifting and subsiding regions are not specified: they are instead lumped together into the value of the parameter ΔT_c as described by Westaway (2001a) and Westaway et al. (2002). Lower-crustal flow forced by a ΔT_c of $-4 \text{ }^\circ\text{C}$ starting at 1.2 Ma is assumed to be supplemented by additional flow with ΔT_c $-5 \text{ }^\circ\text{C}$ starting at 0.9 Ma. However, the combined dimensions of both regions are assumed to be much smaller than the flexural wavelength of the mantle lithos-

exist *a priori* for favouring either of the physical models in Figs 4 or 5. One region that favours Fig. 4 is the Gulf of Corinth in central Greece, investigated by Westaway (1996, 2002b). This is an active normal fault zone where the hanging-wall has evolved since $\sim 0.9 \text{ Ma}$ from being a shallow lacustrine depocentre to a marine depocentre beneath up to $\sim 900 \text{ m}$ of water. On the same time scale, a former (Pliocene to Early Pleistocene) lacustrine depocentre of similar dimensions, located in the footwall, has experienced dramatic uplift and erosion, supplying much of the sediment which has since accumulated in the interior of the Gulf. Westaway (1996, 2002b) has suggested that the start of this erosion was triggered by incision linked to the fall in global sea-level and/or the high rainfall expected during OIS 22 ($\sim 0.87 \text{ Ma}$). The subsequent surface uplift has led to the development of a remarkable sequence of marine and lacustrine terraces along the southern shore of the Gulf (Fig. 9a), the latter forming during glacial stages when a lake develops at the level of a drainage threshold at the western end of the Gulf (Fig. 9b). Fig. 10 shows that a model of the form of Fig. 4, with a single direction of sediment transport, can account for the main features observed in this locality, simultaneously explain-

ing the increase in bathymetry of the depocentre and the time-dependence of uplift of the sediment source, in terms of non-steady-state lower crustal flow with $\eta_c \sim 6 \times 10^{19} \text{ Pa s}$, consistent with a moderate Moho temperature of $\sim 550 \text{ }^\circ\text{C}$. In this particular locality, the effect of cyclic surface loading is smaller than elsewhere, because there has been no significant ice sheet anywhere nearby during any Quaternary glaciation, and because the Gulf of Corinth is bounded by a drainage threshold which prevents its water level dropping below $\sim 60 \text{ m}$ at times of reduced global sea-level. As a result, this effect has been ignored in this modelling. Components of lower-crustal flow out of the plane of section, driven by the sediment loading, or into the plane of section, driven by the pressure-reduction caused by erosion, have also been ignored in this modelling. As is discussed by Westaway (2002b), the main consequence of the simplifying assumption that all induced flow follows the shortest possible path is that the estimate obtained for the lower-crustal effective viscosity is the upper bound to a range of possible values.

A noteworthy feature of these model solutions is that erosion at a rate of 0.2 mm a^{-1} lasting $\sim 1 \text{ Ma}$, and thus involving loss, on average, of a $\sim 200 \text{ m}$ thick lay-

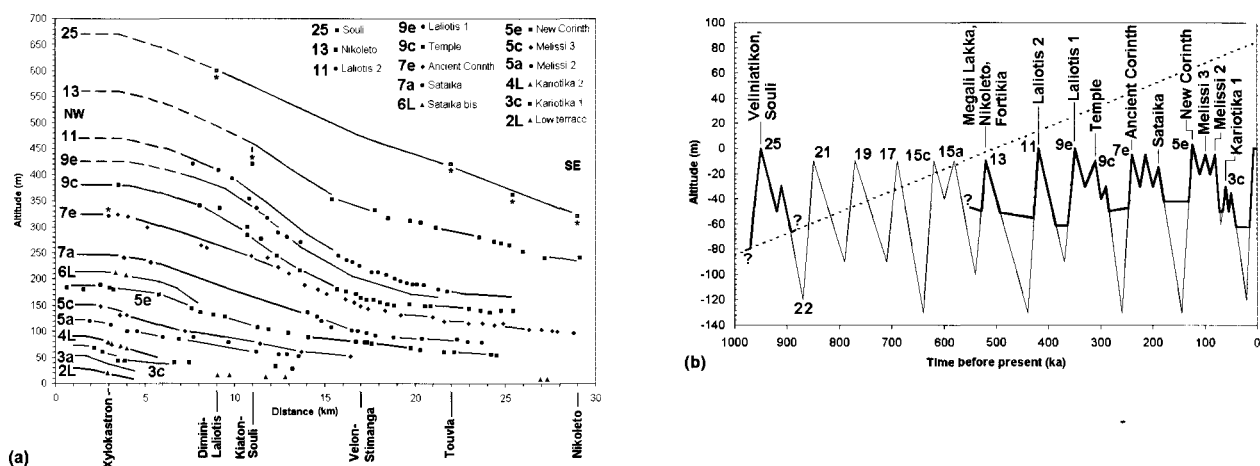


Fig. 9. (a) Terrace profile along the southern shore of the eastern Gulf of Corinth, projected onto a NW-SE line, and showing OIS correlations. Shoreline angle altitude measurements are from Armijo et al. (1996), with additional data, marked *, from Keraudren & Sorel (1987), Keraudren et al. (1995), and Westaway (1996, 2002b). Dashed lines extrapolate the oldest terraces, which are only preserved in the south-east. (b) Summary of Gulf water level for the last million years (thick line), in relation to global sea-level (thin line, labelled with OIS numbers) and the level of the Corinth isthmus col, at the eastern end of the Gulf (dashed line). This diagram updates Westaway (1996, Fig. 6), with minor revisions to timings and magnitudes of global sea-level fluctuations, new terrace nomenclature and age assignments (from Armijo et al., 1996 and Westaway, 2002a), and given the realisation that the Gulf formed a lake in OIS 4 as well as during major glacials (Perissoratis et al., 2000). Dashed line assumes that the Corinth isthmus col uplifted from -80 m before OIS 25 to its present $+75$ m level at a uniform rate, as discussed by Westaway (1996). Estimated lake levels during glacials are based on Westaway's (1996) analysis of present-day levels of their palaeo-shorelines in localities of known uplift rate. ? symbols indicate that, on the time scales indicated, it is unclear whether the Gulf water level followed the global sea-level or a lake existed within it. Adapted from Westaway (2002b, Figs 7 and 8).

er, has driven ~ 700 m of uplift of the oldest marine terrace, and thus ~ 700 - 200 m or ~ 500 m of typical uplift of the eroding land surface. Unlike simple Airy isostatic calculations (e.g., Molnar & England, 1990; Fig. 2), in this type of coupled model involving transient thermal effects, the increase in mean altitude of an eroding land surface may thus substantially exceed the corresponding mean thickness of the layer that is eroded. Likewise, the outflow of lower crust from beneath the Gulf of Corinth depocentre has dynamically created an amount of accommodation space that greatly exceeds the assumed spatial average of ~ 200 m of deposition on the same time scale.

In other regions, cyclic surface loading can be identified as the cause of observed surface uplift. Oxygen isotope studies indicate that northern hemisphere ice sheets grew progressively larger during successive glaciations in the late Early Pleistocene, culminating in OIS 22 with the first glaciation comparable to the largest in the Middle and Late Pleistocene (e.g., Mudelsee & Schulz, 1997). As Westaway (2002a) has noted, forcing of lower-crustal flow by the growth and decay of these Scandinavian ice sheets provides a natural explanation for the abundant river terrace evidence that uplift rates across much of Europe increased at this time. This increase in uplift rates was first recognised by George Kukla in the 1970's (e.g., Kukla, 1975, 1978): he called it the 'K-break', given evidence of increased rates of gorge incision in cli-

mate cycle 'K' (using Kukla's alphabetic notation for climate cycles) that includes OIS 22. The main geomorphological consequence of this event is that many river systems switched around this time from creating broad, shallow valleys to narrow, deeply-incised gorges.

A clear example of this effect is provided by the Middle Rhine gorge through the Rhenish Massif (Fig. 3). From Westaway (2001a), uplift rates in this region were very low – typically ~ 0.04 mm a^{-1} – during the Early Pleistocene, then increased abruptly to a maximum of ~ 0.23 mm a^{-1} in the Middle Pleistocene, with ~ 150 m of gorge incision since OIS 22 (see also Westaway, 2002a). The low Early Pleistocene uplift rate may have resulted from relatively slow erosion of the metamorphic rocks of the Rhenish Massif (see below). In contrast, the subsequent rate was higher than is typical: due to the relatively high mobility of the lower crust in this region caused by its higher-than-usual Moho temperature (the temperature at the base of the mobile lower crust, above a layer of mafic underplating, being estimated by Westaway, 2001, as ~ 640 °C); as well as proximity to the Scandinavian ice margin during glacial maxima, which enhanced the induced lower-crustal flow (Westaway, 2001a). The effective viscosity, η_e , of the lower crust required to sustain uplift at this rate in this region was estimated by Westaway (2001a) as $\sim 10^{18}$ Pa s given the magnitude of horizontal pressure gradients caused by load-

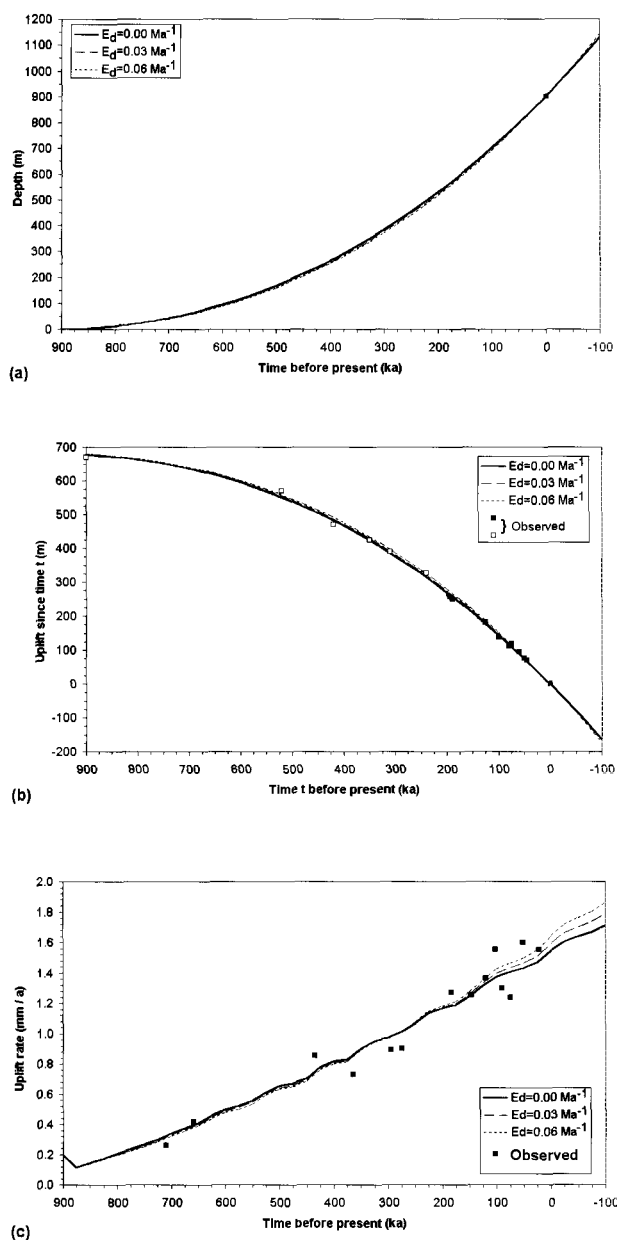


Fig. 10. Results from modelling the Quaternary evolution of the Gulf of Corinth - 1. The predictions are obtained by summing the contributions for each 25 ka time step from the process in Fig. 4. (a) Observed and predicted water depths within the Gulf. (b) and (c) Observed and predicted amounts (b) and rates (c) of uplift of marine terraces in the Xylokastron area south of the Gulf (Fig. 9a). In (b), solid symbols represent the younger marine terraces whose ages and altitudes are well constrained; open symbols indicate the older terraces whose ages are less certain and most of which have to be extrapolated to Xylokastron (Figs 9(a,b)). Calculations assume that sedimentation in the Gulf interior increased from 0.1 mm a^{-1} to 0.2 mm a^{-1} at 0.9 Ma, when the region south of the Gulf changed from being a 0.1 mm a^{-1} depocentre to eroding at 0.2 mm a^{-1} . The Gulf interior and the eroding sediment source are both assumed to be 30 km wide, in crust with a 30 km initial thickness overlain by 70 km thick mantle lithosphere. The isostatic response calculations assume densities of 1000, 2700, 3300, and 3100 kg m^{-3} for water, crust, mantle lithosphere and asthenosphere, and also take account of crustal extension at a strain rate of 0.06 Ma^{-1} (equivalent to $\sim 4 \text{ mm a}^{-1}$ of extension across the 60 km width of the model). For each graph, three alternative solutions are calculated, for E_d (the extensional strain rate taken up by distributed stretching, as opposed to localised slip on normal faults bounding the southern margin of the Gulf) and η_e 0.00 Ma^{-1} and $5.9930 \times 10^{19} \text{ Pa s}$, 0.03 Ma^{-1} and $6.2510 \times 10^{19} \text{ Pa s}$, and 0.06 Ma^{-1} and $6.5085 \times 10^{19} \text{ Pa s}$.

Thames terrace record is one of the best documented worldwide, particularly with regard to biostratigraphic age control for the Middle Pleistocene (e.g., Bridgland, 1994; Preece, 1995; Bridgland & Schreve, 2001). Westaway et al. (2002) have modelled the uplift histories of five sites in south-east England on the Middle and Lower reaches of the Thames. Their results indicate that, since the latest Early Pleistocene (OIS 22), about 60 m of uplift has occurred. This component of uplift appears to be spatially relatively uniform, with only minor lateral variations. In contrast, a much more significant phase of uplift starting at $\sim 3 \text{ Ma}$, and persisting into the Early Pleistocene, was also identified. The uplift during this phase is spatially rather variable: localities near the modern North Sea coastline appear to have been stable or slowly subsiding at this time. Moving west, this early component of uplift increases westward, in the upstream direction, reaching a maximum of $\sim 200 \text{ m}$ along the Middle Thames. Previously, Maddy (1997) investigated the uplift history of one locality beside the Upper Thames: Charlbury, $\sim 20 \text{ km}$ NW of Oxford. He showed that the local river terrace dataset (Fig. 12), which records $\sim 140 \text{ m}$ of incision since $\sim 1.8 \text{ Ma}$, can be explained by surface uplift at a uniform rate of $\sim 0.07\text{--}0.08 \text{ mm a}^{-1}$ throughout this time period.

Fig. 12 shows an alternative attempt at modelling this uplift history, assuming that it results from cyclic surface loading (Fig. 5): an early phase of uplift, starting at $\sim 3 \text{ Ma}$ and concentrated between ~ 3 and ~ 2

ing by Scandinavian ice sheets. Westaway (2001a) also showed that η_e of $\sim 10^{18} \text{ Pa s}$ is reasonable for this region given the temperature distribution in its lower crust, by extrapolation from experimental rock-mechanics data. A further independent estimate of η_e for this region comes from modelling its present-day uplift rates of up to $\sim 2 \text{ mm a}^{-1}$ (observed by repeated surveying over recent decades; Klein et al., 1997) that result from unloading of the crust following large-scale coal mining. Modelling of this uplift by Klein et al. (1997) constrains η_e to between $\sim 3 \times 10^{17} \text{ Pa s}$ and $\sim 10^{18} \text{ Pa s}$.

However, in some other situations, the physical cause of uplift can be much less clear. As an example I consider the uplift history of southern England, deduced from altitudes of Thames river terraces. Following more than a century of investigation, the

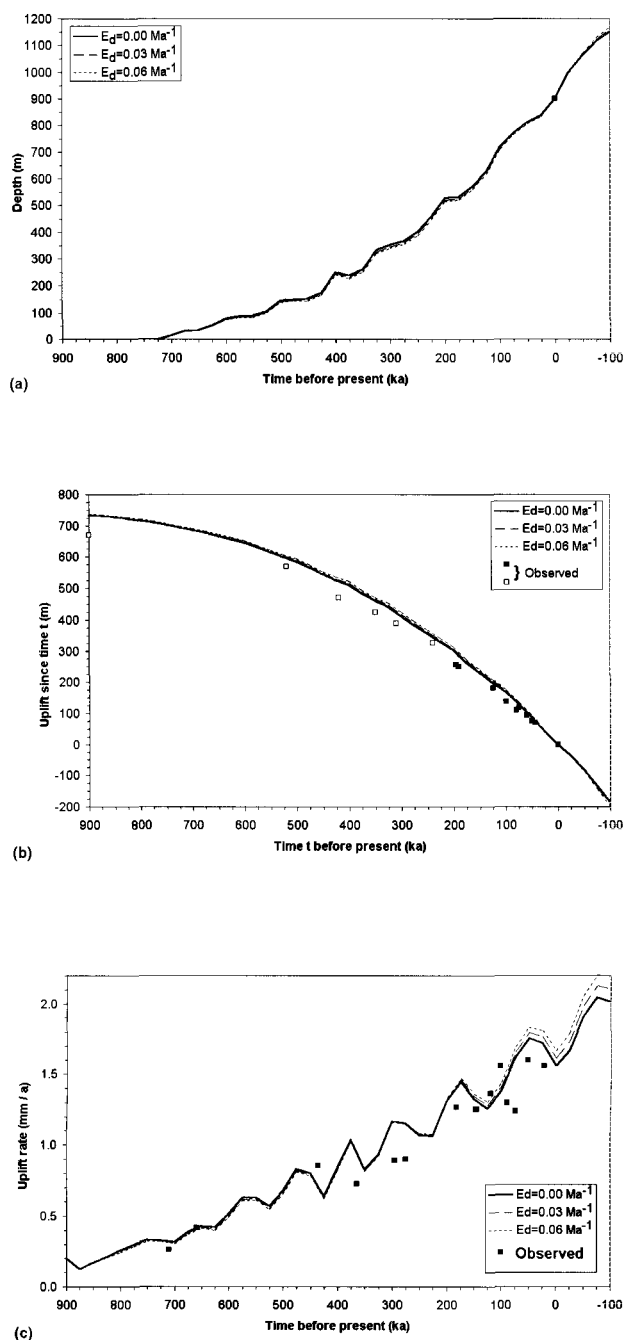


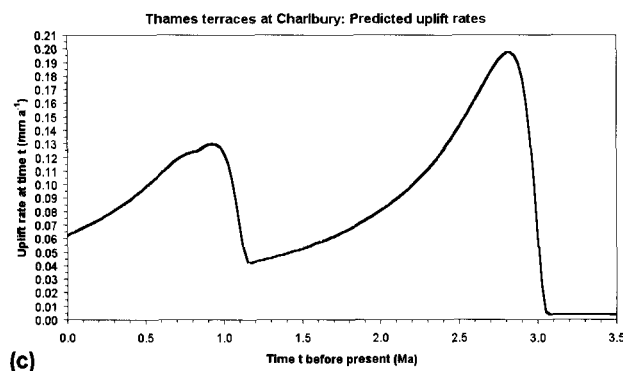
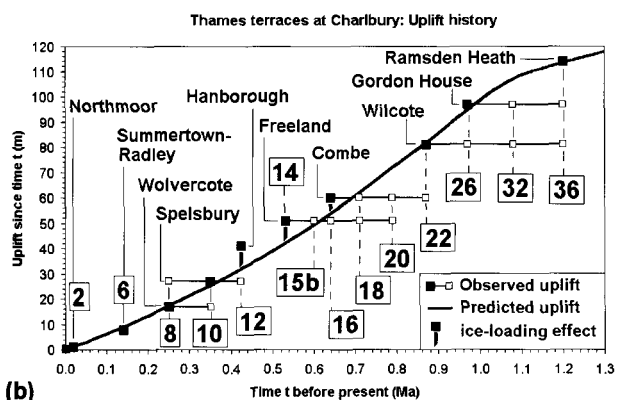
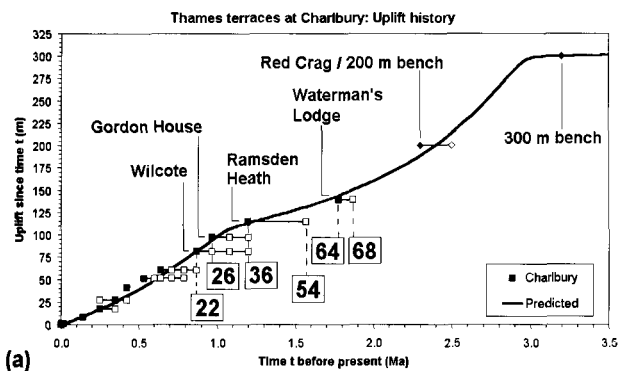
Fig. 11. Results from modelling the Quaternary evolution of the Gulf of Corinth – 2: including variations in water level in accordance with Fig. 9(b). (a) Observed and predicted depths of the Gulf floor below the reference frame provided by present-day global sea-level. The actual water depth will be tens of metres less during many time steps, due to the assumed drawdown in water level (Fig. 9(b)). (b) and (c) Observed and predicted amounts and rates of uplift in the Xylokastron area (Fig. 9(a)). Graphs in (a) (b) and (c) are, respectively, for E_d and η_c 0.00 Ma^{-1} and $5.3854 \times 10^{19} \text{ Pa s}$, 0.03 Ma^{-1} and $5.6140 \times 10^{19} \text{ Pa s}$, and 0.06 Ma^{-1} and $5.8430 \times 10^{19} \text{ Pa s}$. See Fig. 10 caption for notation and calculation procedures.

Ma, resulted in $\sim 140 \text{ m}$ of calculated uplift before $\sim 2 \text{ Ma}$ at rates of up to $\sim 0.2 \text{ mm a}^{-1}$. The subsequent river terrace sequence thus records the gradual tailing-

off of this phase of uplift, plus a second phase starting at $\sim 0.9 \text{ Ma}$. These two uplift phases, with rates varying substantially over time, combine to produce the same total amount of uplift since $\sim 1.8 \text{ Ma}$ as a uniform rate of $\sim 0.08 \text{ mm a}^{-1}$ would have done (Fig. 12). The 3.1 Ma start of forcing of uplift in this model is assumed to relate to effects following the start of upland glaciation in Europe, as is discussed by Westaway (2001a) and Westaway et al. (2002).

Age constraints in Fig. 12 are provided by the Northmoor and Summertown-Radley terrace deposits, which are well-dated (e.g., Maddy et al., 1998; Bridgland & Schreve, 2001) and by the association of gravels of the Hanborough terrace with Anglian age glacial deposits (e.g., Sumbler, 2001) and other reasoning in support of an OIS 12 age (e.g., Maddy & Bridgland, 2000; Bridgland & Schreve, 2001). The Anglian glaciation is indeed assumed here to have ended in OIS 12, not OIS 10 as Sumbler (2001) thought. Indirect age constraints on the older terraces result from correlating the Wilcote (or North Leigh) terrace with the Beaconsfield / Bures terrace of the Middle and Lower Thames (e.g., Bridgland, 1994), and the Waterman's Lodge terrace with the Stoke Row terrace farther downstream. Preferred ages of OIS 22 and 64, respectively, are deduced for these downstream correlatives (Westaway et al., 2002; Westaway, 2002a). The other river terraces are assigned to oxygen isotope stages by interpolation. The only constraint on the early part of this uplift history, discussed by Maddy et al. (2001), is provided by poorly-defined erosion surfaces at ~ 200 and $\sim 300 \text{ m}$ altitudes. These form the summits of hills that rise above the general landscape level in this region, and are thought to represent fragments of marine wavecut platforms that date from $\sim 2.5 \text{ Ma}$ and before $\sim 3 \text{ Ma}$. The '300-m' platform is thus tentatively regarded as marking the conditions of relative stability that existed before the start of rapid uplift forcing at $\sim 3 \text{ Ma}$. This example thus illustrates an important point: in order to physically model this detailed Early-Middle Pleistocene river terrace record, one needs to know the starting conditions that existed when uplift began in the Late Pliocene. This unavoidably requires the use of the poorly defined (and thus, of controversial significance) landscape evidence that exists from beforehand.

The Thames drainage catchment is situated within relatively cold continental crust of the London Platform, which accreted in the Late Precambrian and has since remained virtually stable (see Westaway et al., 2002, for more detail), with a Moho temperature probably not much greater than 500°C . The present land surface in this region is in rock ranging in age



from Jurassic to Palaeogene, much of which is unlithified – a consequence of the rocks never having experienced deep burial. Westaway et al. (2002) showed that the observed ~60 m of uplift in this region since OIS 22 is about the maximum that is feasible as a result of the process in Fig. 5, given the high effective viscosity of the crust in this region and the likely order-of-magnitude of pressure-gradients resulting from ice-loading in adjacent regions during glacial maxima on this time scale.

However, given the much smaller ice loads that existed during cold stages before OIS 22, and the resulting much smaller pressure gradients that they would induce in the lower crust, there is no way that the mechanism in Fig. 5 can have generated fast enough inflow into the high-viscosity lower crust beneath southern England to sustain the much higher uplift

Fig. 12. Results from modelling the Quaternary uplift history at Charlbury, beside the Upper Thames river in central-southern England: the post-Middle Pliocene uplift history (a); an enlargement of the most recent part of this uplift history (b); and the corresponding history of uplift rate variations (c). Altitude data for tops of river terraces, which range at this locality from 60 to 198 m above sea-level, are from Maddy (1997) (see also Maddy et al., 2001) and Sumbler (2001). ‘Observed’ uplift in (a) and (b) is estimated from these river terrace altitudes by assuming that the Upper Thames develops an equivalent quasi-equilibrium profile each time a terrace forms, with the top of each terrace forming at a contemporaneous altitude of 59 m relative to global sea-level. This means that the channel length changes and diversions which have occurred on the Lower Thames (e.g., Maddy et al., 2000; Westaway et al., 2002) are assumed to not affect this study locality as it is so far upstream. Solid symbols indicate my preferred assignments of terraces to oxygen isotope stages; open circles indicate other alternatives; marine features being indicated using different ornament. Predicted uplift is calculated for lower-crustal flow concentrated at 29 km depth in lower crust with the base of the brittle layer initially at 21 km depth, a geothermal gradient of $10^{\circ}\text{C km}^{-1}$, and a thermal diffusivity of $1.2 \times 10^{-6} \text{ m}^2 \text{ s}^{-1}$. Four phases of forcing by cyclic surface loads (Fig. 5) are assumed, starting at 18 Ma ($\Delta T_e -6^{\circ}\text{C}$), 3.1 Ma ($\Delta T_e -3.5^{\circ}\text{C}$), 1.2 Ma ($\Delta T_e -1.7^{\circ}\text{C}$), and 0.9 Ma ($\Delta T_e -0.2^{\circ}\text{C}$).

rates depicted in Fig. 12 for the Late Pliocene and earliest Pleistocene. If this mechanism is thus eliminated as the cause of this early phase of uplift, the possibility emerges that it was instead caused by an increase in erosion rates (Fig. 4). If so, it follows that much of the present landscape of southern England may have typically been buried in the Late Pliocene beneath a layer – maybe ~100 m thick – of other rocks, younger than the present-day outcrop in each locality. If so, and this layer was eroded during the early stages of climate deterioration before ~2 Ma, the resulting isostatic response could have driven the early phase of uplift evident in Fig. 12. The curve in Fig. 12 is – of course – calculated for the response to cyclic surface loading, not non-steady-state erosion. However, given the similarity in these responses, evident in Fig. 8, it is likely that an erosion rate history will exist, involving an increase around 3 Ma and then a subsequent decrease to near zero around 2 Ma, that will give a similar predicted uplift history. The main physical evidence in support of such an erosion history is the presence at many localities in southern England of shallow marine sediments of Pliocene age (the Lenham Beds and Red Crag) at altitudes of up to ~200 m – either as small outcrops or within solution pipes (see Westaway et al., 2002, for a review of this evidence) – suggesting that more extensive cover of a similar character formerly existed.

Other possible supporting evidence for this general form of erosion history is provided by the sedimentary record offshore of southern and western Britain. This record (e.g., Pantin & Evans, 1984; Evans, 1990;

Tappin et al., 1994) reveals widespread clastic sediment from the Late Pliocene and earliest Pleistocene, indicating contemporaneous erosion on this time scale, but typically very little younger sediment except for material deposited in the most recent climate cycle (and which may well be eroded during the next fall in sea-level). Jones (1999) indeed suggested that in the Late Pliocene the land surface of south-east England was covered by a deeply-weathered 'regolith' that was rapidly eroded following the initial deterioration in climate, since when rates of erosion have decreased. The proposed hypothetical 'pulse' of rapid erosion during ~3 to ~2 Ma also provides a natural explanation for the absence of river terraces preserved from before ~2 Ma in southern England, in contrast with other regions such as the Netherlands and Germany (e.g., Westaway, 2001a). It may also explain why field evidence of older marine shoreline features is so obscure and fragmentary: these features would have typically been obliterated as the land surface eroded – before ~2 Ma – to a lower level, and so could only be preserved in localities that happened not to erode significantly at this time. The oldest river terraces in southern England, which formed at or just after ~2 Ma, such as the Watermans Lodge terrace on the Upper Thames (Fig. 12a) and the slightly older Nettlebed terrace of the Middle Thames (e.g., Bridgland, 1994) indeed occur close to the highest points in the modern landscape, consistent with this hypothesis of rapid erosion before ~2 Ma but little or no erosion since.

Fig. 12(b) also illustrates the consequences of an additional physical process that can affect altitudes of river terraces: the direct effect of ice loading. Maddy & Bridgland (2000), Westaway et al. (2002), and Westaway (2002a) have pointed out that along the Middle Thames, adjacent to the Anglian (OIS 12) ice margin, the top of the Winter Hill terrace that aggraded while this ice was present is at least ~15 m higher than would be expected from altitudes of other terraces in the sequence. This is interpreted as a consequence of this terrace having formed while the adjacent crust was loaded by the Anglian ice sheet. When this ice load was removed, this terrace and the underlying crust are thus regarded as having rapidly rebounded to their present relative level. At Charlbury (Fig. 12b), this effect can also explain why the Hanborough (OIS 12) terrace is ~9 m higher than expected. The older Combe and Freeland terraces may also indicate the same effect. Fig. 12(b) indicates that the Combe terrace could have formed in OIS 18 with no ice loading (as suggested by Westaway et al., 2002, and Westaway, 2002a), or in OIS 16 with ~6 m of ice loading. Likewise, the Freeland terrace could have

formed in OIS 16 or 15b with no ice loading, or in OIS 14 with ~9 m of ice loading, or even in OIS 12 (shortly before the Hanborough terrace) with ~19 m of ice loading.

Post-glacial rebound effects such as these have previously been modelled by many people as a result of flow in the asthenosphere, the crust and mantle lithosphere being assumed to form an elastic layer on the time scale of ~10–20 ka required for the resulting isostatic response. The range of possible effective viscosities for the lower crust, suggested in this study, includes values much lower than any conceivable viscosity in the asthenosphere (e.g., Westaway et al., 2002). This study has indeed shown that these low viscosities, estimated for lower crustal temperatures, are consistent for loading in laboratory experiments (carried out on time scales of months or less), for unloading due to mining (over decades), and for cyclic loading spanning many climate cycles (over hundreds of thousands of years). It is thus expected that other loading processes, operating on time scales that are intermediate between these limits, such as post-glacial rebound (over thousands to tens of thousands of years) and sea-level fluctuations (over centuries to millennia), will in reality be accommodated by flow in the lower crust as well as, or instead of, in the asthenosphere.

The present modelling strategy (Fig. 5) does not incorporate the direct effect of ice loading, its existence being instead revealed by mismatch between observed uplift histories and model predictions (as in Fig. 12(b)): the scheme in Fig. 5 only considers the associated indirect thermal effects resulting from the induced lower-crustal flow. The computer program used to implement the modelling technique in Fig. 5 simply does not calculate the transient lower-crustal flow patterns that will occur on the very short term time-scales relevant to investigating these loading effects. Such post-glacial rebound will of course be balanced by loading during the preceding ice-accumulation phase, such that overall, throughout any climate cycle, its direct net effect on surface uplift will be zero. This program in its present form thus cannot be used to analyse effects such as water loading in coastal localities due to the Flandrian transgression, or uplift in formerly glaciated areas experiencing post-glacial rebound due to ice unloading in the past 10–20 ka.

Although the computer program used to implement the modelling technique illustrated in Fig. 4 also has limited time resolution, it can provide a crude indication of the effect of water-loading fluctuations, superposed onto the effects of non-steady-state erosion, as in Fig. 11. Comparison of Fig. 11(a) and Fig.

10(a) indicates that water-loading effects cause the level of the floor of the Gulf of Corinth to fluctuate by up to several tens of metres on either side of the smoother pattern that occurs when only effects of non-steady-state erosion are considered.

Because the present modelling assumes that the rheology of the crust, and thus its response to each loading process, is linear (see earlier discussion, also Westaway, 1998), processes operating on different time scales can be treated separately. For instance, abundant evidence indicates that the crust in many coastal localities in southern England has *subsided* relative to sea-level by varying distances, typically several metres, during the Holocene marine high-stand (e.g., Shennan, 1989; Long, 1992, 1995; Haggart, 1995; Long & Tooley, 1995; Long et al., 2000), even though the presence of river terrace staircases indicates that many of the same localities have *uplifted* throughout the Quaternary (e.g., Bridgland, 1994; Westaway et al., 2002). However, there is no contradiction between these observations indicating different net rates and senses of vertical crustal motions on different time scales. Reasons for the overall net uplift throughout the Quaternary have been well-explained. The Holocene subsidence of the crust is presumably the direct response to water loading following the Flandrian transgression (analogous to the ripple along the curve in Fig. 11c, which results from the same effect): subsidence being expected at any site within half a flexural wavelength (equation (3)) of any part of this water load. The local variations in this subsidence presumably reflect differences in the coastal geometry between localities, which influence amounts of water loading in the vicinity, the loading being accommodated by outflow of lower crust at depth. Compared with the Gulf of Corinth, southern England of course responds to larger-amplitude water-level fluctuations, but the crust has a higher effective viscosity (see Westaway et al., 2002) and the coastline shelves much more gently, with much smaller water depths typically present within a given distance of the coastline. On the other hand, the upper-crustal brittle layer is typically thicker in southern England (cf. Westaway et al., 2002), so its flexural wavelength will be longer (equation (3)), and a greater adjacent surface area and volume of water load will contribute to loading each point on the coastline than for the Gulf of Corinth. It is not obvious at this stage how these different effects will trade against each other to give the magnitude of the water-loading effect on lower-crustal flow for southern England, or any other locality. The development of numerical methods specifically intended for modelling post-glacial rebound and/or Holocene sea-level fluctuations as a consequence of lower-crustal

flow can thus be identified as an important research objective for the future, but it is beyond the scope of this present study.

Conclusions

Lower crustal flow, induced by cyclic surface loading (Fig. 5) and/or non-steady-state erosion (Fig. 4), can cause thickening of the continental crust resulting in surface uplift. However, the predicted form of the response to both processes can be very similar, which can make it difficult to resolve which process is occurring in any region, unless one has evidence of the regional conditions before uplift began. Strategies for modelling both processes have been summarised. They are based on the assumption of a low flexural rigidity in the brittle upper crust and a linear rheology for the plastic lower crust with viscosity dependent on temperature but not on strain rate. Flow in the lower crust is assumed to be driven by pressure variations at the base of the brittle layer induced by surface processes, taking account of vertical advection of this thermal boundary that occurs relative to the rock column due to the resulting non-steady thermal state of the crust.

It is suggested that cyclic surface loading, caused by the growth and decay of continental ice sheets and the associated sea-level fluctuations, is the main cause of the increase in uplift rates in the early Middle Pleistocene: it follows the increase in scale of ice sheet development from OIS 22 onwards. This increase in uplift rates is widely-recognised from river terrace records, and typically marks a transition from broad valleys in areas of low relief to narrower, more deeply incised gorges. The less well resolved earlier increase in uplift rates, evident in some river terrace records at ~3 Ma, is more likely to result from the isostatic response to increased rates of erosion linked to the contemporaneous deterioration in climate.

Acknowledgements

I thank David Bridgland and David Petley for thoughtful and constructive reviews. This study is a contribution to International Geological Correlation Programme 449 'Global Correlation of Late Cenozoic fluvial deposits'.

References

- Arger, J., Mitchell, J. & Westaway, R., 2000. Neogene and Quaternary volcanism of south-eastern Turkey. *In*: Bozkurt, E., Winchester, J.A. & Piper, J.D.A. (eds): *Tectonics and Magmatism of Turkey and the Surrounding Area*. Geological Society of London Special Publication 173: 459-487.

- Armijo, R., Meyer, B., King, G.C.P., Rigo, A. & Papanastassiou, D., 1996. Quaternary evolution of the Corinth Rift and its implications for the Late Cenozoic evolution of the Aegean. *Geophysical Journal International* 126: 11-53.
- Bond, G., 1978. Evidence for Late Tertiary uplift of Africa relative to North America, South America, Australia and Europe. *Journal of Geology* 86: 47-65.
- Bridgland, D.R., 1994. The Quaternary of the Thames. Nature Conservancy Council (London, England): 441 pp.
- Bridgland, D.R. & Allen, P., 1996. A revised model for terrace formation and its significance for the early Middle Pleistocene terrace aggradations of north-east Essex, England. *In: Turner, C. (ed.): The early Middle Pleistocene in Europe*. Balkema (Rotterdam): 121-134.
- Bridgland, D.R. & Schreve, D.C., 2001. River terrace formation in synchrony with long-term climatic fluctuation: examples from southern Britain. *In: Maddy, D., Macklin, M. & Woodward, J. (eds): River Basin Sediment Systems: Archives of Environmental Change*. Balkema (Abingdon, England): 229-248.
- Buck, W.R., 1988. Flexural rotation of normal faults. *Tectonics* 7: 959-973.
- Cheremisinoff, N.P., 1993. *An Introduction to Polymer Rheology and Processing*, CRC Press (Ann Arbor, Michigan).
- Cross, M.M., 1966. Rheology of non-newtonian fluids: A new flow equation for pseudoplastic systems. *Journal of Colloid Science* 20: 417-437.
- Damon, P.E., 1971. The relationship between Late Cenozoic volcanism and tectonism and orogenic-epi-orogenic periodicity. *In: Turekian, K.E. (ed.), The Late Cenozoic Glacial Ages*. Yale University Press (New Haven, Connecticut): 15-35.
- De Sitter, L.U., 1952. Pliocene uplift of Tertiary mountain chains. *American Journal of Science* 250: 297-307.
- England, P. & Molnar, P., 1990. Surface uplift, uplift of rocks, and exhumation of rocks. *Geology* 18: 1173-1177.
- Evans, C.D.R., 1990. The geology of the western English Channel and its western approaches. British Geological Survey UK Off-shore Regional Report. Her Majesty's Stationary Office (London, England): 93 pp.
- Eyles, N., 1996. Passive margin uplift around the North Atlantic region and its role in northern hemisphere late Cenozoic glaciation. *Geology* 24: 103-106.
- Flint, R.F., 1957. *Glacial and Pleistocene Geology*. John Wiley & Sons (London, England): 553 pp.
- Geyl, W.F., 1960. Geophysical speculations on the origin of stepped erosion surfaces. *Journal of Geology* 68: 154-176.
- Gilchrist, A.R., Kooi, H. & Beaumont, C., 1994. Post-Gondwana evolution of southwestern Africa: Implications for the controls on landscape development from observations and numerical experiments. *Journal of Geophysical Research* 99: 12,211-12,228.
- Gilchrist, A.R. & Summerfield, M.A., 1990. Differential denudation and flexural isostasy in the formation of rifted-margin upwarps. *Nature* 346: 739-742.
- Gilchrist, A.R., Summerfield, M.A. & Cockburn, H.A.P., 1991. Landscape dissection, isostatic uplift, and the morphologic development of orogens. *Geology* 22: 963-966.
- Greene, M.T., 1982. *Geology in the Nineteenth Century: Changing Views of a Changing World*. Cornell University Press (Ithaca, New York): 324 pp.
- Haggart, B.A., 1995. A re-examination of some data relating to Holocene sea-level changes in the Thames estuary. *In: Bridgland, D.R., Allen, P. & Haggart, B.A. (eds): The Quaternary of the Lower Reaches of the Thames, Field Guide*. Quaternary Research Association (Durham, England): 329-337.
- Herschel, J.F.W., 1837. Letter to Lyell. *In: Babbage, C. (ed.): On the Action of Existing Causes in Producing Elevations and Subsidences in Portions of the Earth's Crust*. The Ninth Bridgewater Treatise, Appendix G. John Murray (London, England): 202-217.
- Holmes, A., 1965. *Principles of Physical Geology*, 2nd edition, Nelson (London, England): 1288 pp.
- Jones, D.K.C., 1999. Evolving models of the Tertiary evolutionary geomorphology of southern England, with special reference to the Chalklands. *In: Smith, B.J., Whalley, W.B. & Warke, P.A. (eds): Uplift, Erosion, and Stability: Perspectives on Long-term Landscape Development*. Geological Society of London Special Publication 162: 1-23.
- Kaufman, P.S. & Royden, L.H., 1994. Lower crustal flow in an extensional setting: Constraints from the Halloran Hills region, eastern Mojave Desert, California. *Journal of Geophysical Research* 99: 15723-15739.
- Keraudren, B., Falguères, C., Bahain, J.-J., Sorel, D. & Yokoyama, Y., 1995. New radiometric dating from the marine terraces of Corinthia, Greece. *Comptes Rendus de l'Académie des Sciences de Paris, Series IIA* 320: 483-489 (in French with English summary).
- Keraudren, B. & Sorel, D., 1987. The terraces of Corinth (Greece) - a detailed record of eustatic sea-level variations during the last 500,000 years. *Marine Geology* 77: 99-107.
- King, L.C., 1955. Pediplanation and isostasy: An example from South Africa. *Quarterly Journal of the Geological Society of London* 111: 353-359.
- King, G.C.P. & Ellis, M.A., 1990. The origin of large local uplift in extensional regions. *Nature* 348: 689-693.
- King, G.C.P., Stein, R.S. & Rundle, J.B., 1988. The growth of geological structures by repeated earthquakes, 1. Conceptual framework. *Journal of Geophysical Research* 93: 13307-13318.
- Klein, A., Jacoby, W. & Smilde, P., 1997. Mining-induced crustal deformation in northwest Germany: modelling the rheological structure of the lithosphere. *Earth and Planetary Science Letters* 147: 107-123.
- Kooi, H. & Beaumont, C., 1994. Escarpment evolution on high-elevation rifted margins: Insights derived from a surface processes model that combines diffusion, advection, and reaction. *Journal of Geophysical Research* 99: 12191-12209.
- Kooi, H., Hettema, M. & Cloetingh, S., 1991. Lithospheric dynamics and the rapid Pliocene-Quaternary subsidence phase in the southern North Sea basin. *Tectonophysics* 192: 245-259.
- Kukla, G.J., 1975. Loess stratigraphy of central Europe. *In: Butzer, K.W. & Isaac, G.L. (eds): After the Australopithecines* (Mouton, The Hague): 99-188.
- Kukla, G.J., 1978. The classical European glacial stages: correlation with deep-sea sediments. *Transactions of the Nebraska Academy of Sciences* 6: 57-93.
- Kuszniir, N.J. & Park, R.G., 1984. Continental lithosphere strength: the critical role of lower crustal deformation. *In: Dawson, J.B., Carswell, D.A. & Wedepohl, K.H. (eds): The Nature of the Lower Continental Crust*. Geological Society of London Special Publication 24: 79-93.
- Kuszniir, N.J., Marsden, G. & Egan, S., 1991. A flexural-cantilever simple-shear / pure-shear model of continental extension: application to the Jeanne d'Arc basin, Grand Banks, and Viking Graben, North Sea. *In: Roberts, A.M., Yielding, G. & Freeman, B. (Eds): The Geometry of Normal Faults*. Geological Society of London Special Publication 56: 41-60.
- Long, A.J., 1995. Sea-level and crustal movements in the Thames estuary, Essex and east Kent. *In: Bridgland, D.R., Allen, P. & Haggart, B.A. (eds): The Quaternary of the Lower Reaches of the Thames, Field Guide*. Quaternary Research Association (Durham, England): 99-105.
- Long, A.J. & Tooley, M.J., 1995. Holocene sea-level and crustal

- movements in Hampshire and Southeast England, United Kingdom. *In: Holocene Cycles: Climate, Sea Levels, and Sedimentation*. Journal of Coastal Research, Special Issue 17: 299-310.
- Long, A.J., Scaife, R.G. & Edwards, R.J., 2000. Stratigraphic architecture, relative sea-level, and models of estuary development in southern England: new data from Southampton Water. *In: Pye, K. & Allen, J.R.L.* (eds): Coastal and Estuarine Environments: Sedimentology, Geomorphology and Geoarchaeology. Geological Society of London Special Publication 175: 253-279.
- Luan, F.C. & Paterson, M.S., 1992. Preparation and deformation of synthetic aggregates of quartz. Journal of Geophysical Research 97: 301-320.
- Lucchitta, I., 1979. Late Cenozoic uplift of the southwestern Colorado Plateau and adjacent lower Colorado River region. Tectonophysics 61: 63-95.
- Maddy, D., 1997. Uplift-driven valley incision and river terrace formation in southern England. Journal of Quaternary Science 12: 539-545.
- Maddy, D. & Bridgland, D.R., 2000. Accelerated uplift resulting from Anglian glacioisostatic rebound in the Middle Thames valley, UK?: Evidence from the river terrace record. Quaternary Science Reviews 19: 1581-1588.
- Maddy, D., Bridgland, D.R. & Green, C.P., 2000. Crustal uplift in southern England: Evidence from the river terrace records. Geomorphology 33: 167-181.
- Maddy, D., Bridgland, D.R. & Westaway, R., 2001. Uplift-driven valley incision and climate-controlled river terrace development in the Thames valley, UK. Quaternary International 79: 23-36.
- Maddy, D., Lewis, S.G., Scaife, R.G., Bowen, D.Q., Coope, G.R., Green, C.P., Hardaker, T., Keen, D.H., Rees-Jones, J., Parfitt, S. & Scott, K., 1998. The Upper Pleistocene deposits at Cassington, near Oxford, England. Journal of Quaternary Science 13: 205-231.
- McKee E.D. & McKee, E.H., 1972. Pliocene uplift of the Grand Canyon region - Time of drainage adjustment. Geological Society of America Bulletin 83: 1923-1932.
- Mitchell, J. & Westaway, R., 1999. Chronology of Neogene and Quaternary uplift and magmatism in the Caucasus: Constraints from K-Ar dating of volcanism in Armenia. Tectonophysics 304: 157-186.
- Molnar, P. & England, P., 1990. Late Cenozoic uplift of mountain ranges and global climate change: Chicken or egg? Nature 346: 29-34.
- Mudelsee, M. & Schulz, M., 1997. The Mid-Pleistocene climate transition: onset of 100 ka cycle lags ice volume build-up by 280 ka. Earth and Planetary Science Letters 151: 117-123.
- Pantin, H.M. & Evans, C.D.R., 1984. The Quaternary history of the central and southwestern Celtic Sea. Marine Geology 57: 259-293.
- Partridge, T.C. & R.R. Maud, 1987. Geomorphic evolution of southern Africa since the Mesozoic. South African Journal of Geology 90: 179-208.
- Pazzaglia, F.J. & Gardner, T.W. 1994. Late Cenozoic flexural deformation of the middle U.S. Atlantic passive margin. Journal of Geophysical Research 99: 12143-12157.
- Perissoratis, C., Piper, D.J.W. & Lykousis, V., 2000. Alternating marine and lacustrine sedimentation during late Quaternary in the Gulf of Corinth rift basin, central Greece. Marine Geology 167: 391-411.
- Preece, R.C., 1995. Mollusca from interglacial sediments at three critical sites in the Lower Thames. *In: Bridgland, D.R., Allen, P. & Haggart, B.A.* (Eds): The Quaternary of the Lower Reaches of the Thames, Field Guide. Quaternary Research Association (Durham, England): 55-60.
- Ranalli, G., 1987. Rheology of the Earth: Deformation and Flow Processes in Geophysics and Geodynamics. Allen & Unwin (London, England): 366 pp.
- Shackleton, N.J., Berger, A. & Peltier, W.R., 1990. An alternative astronomical calibration of the lower Pleistocene timescale based on ODP site 677. Transactions of the Royal Society of Edinburgh, Earth Sciences 81: 251-261.
- Shennan, I., 1989. Holocene crustal movements and sea-level changes in Great Britain. Journal of Quaternary Science 4: 77-89.
- Sibrava, V., 1972. The position of Czechoslovakia in the correlation system of the European Pleistocene. Sbornik Geologických Ved Anthropozoikum, series A 8: 5-218 (in German with English summary).
- Sibson, R.H., 1982. Fault zone models, heat flow, and the depth distribution of earthquakes in the continental crust of the United States. Bulletin of the Seismological Society of America 72: 151-163.
- Smith, B.J., Whalley, W.B. & Warke, P.A., 1999. Uplift, Erosion, and Stability: Perspectives on Long-term Landscape Development. Geological Society of London Special Publication 162.
- Stüwe, K., White, L. & Brown, R., 1994. The influence of eroding topography on steady-state isotherms. Application to fission track analysis. Earth and Planetary Science Letters 124: 63-74.
- Sumbler, M.G., 2001. The Moreton Drift: a further clue to glacial chronology in central England. Proceedings of the Geologists' Association 112:13-27.
- Summerfield, M.A. & Kirkbride, M.P., 1992. Climate and landscape response. Nature 355: 306.
- Tappin, D.R., Chadwick, R.A., Jackson, A.A., Wingfield, R.T.R. & Smith, N.J.P., 1994. The geology of Cardigan Bay and the Bristol Channel. British Geological Survey UK Offshore Regional Report. Her Majesty's Stationery Office (London, England): 107 pp.
- Turcotte, D.L. & Schubert, G., 1982. Geodynamics: Applications of Continuum Physics to Geological Problems. John Wiley & Sons (New York, New York): 450 pp.
- Van den Berg, M.W., 1996. Fluvial sequences of the Maas: a 10 Ma record of neotectonics and climate change at various time-scales. Ph.D. Thesis, University of Wageningen, The Netherlands: 181 pp.
- Van den Berg, M.W. & Van Hoof, T., 2001. The Maas terrace sequence at Maastricht, SE Netherlands: evidence for 200 m of late Neogene and Quaternary surface uplift. *In: Maddy, D., Macklin, M.G. & Woodward, J.C.* (eds): River Basin Sediment Systems: Archives of Environmental Change. Balkema (Abingdon, England): 45-86.
- Veldkamp, A., 1996. Late Cenozoic landform development in East Africa: The role of near base level planation within the dynamic etchplanation concept. Zeitschrift für Geomorphologie, Neue Folge, Supplement 106: 25-40.
- Westaway, R., 1990. Present-day kinematics of the plate boundary zone between Africa and Europe, from the Azores to the Aegean. Earth and Planetary Science Letters 96: 393-406.
- Westaway, R., 1992a. Analysis of tilting near normal faults using calculus of variations: Implications for upper-crustal stress and rheology. Journal of Structural Geology 14: 857-871.
- Westaway, R., 1992b. Seismic moment summation for historical earthquakes in Italy: tectonic implications. Journal of Geophysical Research 97: 15437-15464.
- Westaway, R., 1994a. Reevaluation of extension in the Pearl River Mouth basin, South China Sea: Implications for continental lithosphere deformation mechanisms. Journal of Structural Geology 16: 823-838.
- Westaway, R., 1994b. Evidence for dynamic coupling of surface processes with isostatic compensation in the lower crust during

- active extension of western Turkey. *Journal of Geophysical Research* 99: 20203-20223.
- Westaway, R., 1995. Crustal volume balance during the India-Eurasia collision and altitude of the Tibetan plateau: a working hypothesis. *Journal of Geophysical Research* 100: 15173-15194.
- Westaway, R., 1996. Quaternary elevation change in the Gulf of Corinth of central Greece. *Philosophical Transactions of the Royal Society of London, Series A* 354: 1125-1164.
- Westaway, R., 1998. Dependence of active normal fault dips on lower-crustal flow regimes. *Journal of the Geological Society of London* 155: 233-253.
- Westaway, R., 1999. The mechanical feasibility of low-angle normal faulting. *Tectonophysics* 308: 407-443.
- Westaway, R., 2001. Flow in the lower continental crust as a mechanism for the Quaternary uplift of the Rhenish Massif, north-west Europe. *In: Maddy, D., Macklin, M.G., Woodward, J.C. (Eds): River Basin Sediment Systems: Archives of Environmental Change*. Balkema (Abingdon, England): 87-167.
- Westaway, R., 2002a. Long-term river terrace sequences: Evidence for global increases in surface uplift rates in the Late Pliocene and early Middle Pleistocene caused by flow in the lower continental crust induced by surface processes. *Netherlands Journal of Geosciences*, this volume.
- Westaway, R., 2002b. The Quaternary evolution of the Gulf of Corinth, central Greece: coupling between surface processes and flow in the lower continental crust. *Tectonophysics*, submitted.
- Westaway, R., 2002c. Seasonal seismicity of northern California ahead of the great 1906 earthquake. *Pure and Applied Geophysics*, in press.
- Westaway, R., Maddy, D. & Bridgland, D.R., 2002. Flow in the lower continental crust as a mechanism for the Quaternary uplift of southeast England: constraints from the Thames terrace record. *Quaternary Science Reviews*, 21: 569-603.
- Whorlow, R.W., 1992. *Rheological Techniques*, 2nd edition, Ellis Horwood (New York, New York).